Function Induction and Task Generalization: An Interpretability Study with Off-by-One Addition

Qinyuan Ye **Robin Jia** **Xiang Ren**
University of Southern California
{qinyuany, robinjia, xiangren}@usc.edu

Abstract

Large language models demonstrate the intriguing ability to perform unseen tasks via in-context learning. However, it remains unclear what mechanisms inside the model drive such task-level generalization. In this work, we approach this question through the lens of off-by-one addition (*i.e.*, 1+1=3, 2+2=5, 3+3=?), a two-step, counterfactual task with an unexpected +1 function as a second step. Leveraging circuit-style interpretability techniques such as path patching, we analyze the models' internal computations behind their performance and present three key findings. First, we uncover a function induction mechanism that explains the model's generalization from standard addition to off-by-one addition. This mechanism resembles the structure of the induction head mechanism found in prior work and elevates it to a higher level of abstraction. Second, we show that the induction of the +1 function is governed by multiple attention heads in parallel, each of which emits a distinct piece of the +1 function. Finally, we find that this function induction mechanism is reused in a broader range of tasks, including synthetic tasks such as shifted multiple-choice QA and algorithmic tasks such as base-8 addition. Overall, our findings offer deeper insights into how reusable and composable structures within language models enable task-level generalization.[1]

1 Introduction

As the capabilities of language models (LMs) continue to grow, users apply them to increasingly challenging and diverse tasks, accompanied by evolving expectations (Zhao et al., 2024; Tamkin et al., 2024; Kwa et al., 2025). Consequently, it becomes impractical to include every task of interest in a model's training prior to deployment. In this context, task-level generalization—the ability of a model to perform novel tasks at inference time—becomes highly crucial and valued.

Prior work shows that LMs already exhibit this capability to a significant extent through in-context learning (Brown et al., 2020; Chen et al., 2022; Min et al., 2022a). The underlying mechanisms of this behavior are being actively investigated, with work on induction heads (Olsson et al., 2022) and function vectors (Hendel et al., 2023; Todd et al., 2024) offering substantial insights. However, our understanding is still limited, especially regarding more complex generalization scenarios involving unexpected elements or newly defined concepts in the task.

In this work, we aim to enhance our understanding of how models handle novelty and unconventionality with one counterfactual task: off-by-one addition (*i.e.*, 1+1=3, 2+2=5, 3+3=?). For humans, this task consists of two sequential steps: standard addition, followed by an unexpected increment of one to the sum. When a language model is prompted to perform this task with in-context learning, we anticipate two possible outcomes: (1) the model acquires the intended +1 operation and thus outputs 7, or (2) it adheres to fundamental arithmetic rules and outputs 6.

[1]Code: INK-USC/function-induction

39th Conference on Neural Information Processing Systems (NeurIPS 2025) Workshop: Mechanistic Interpretability.

We begin our study by evaluating six contemporary LMs on off-by-one addition. Our findings indicate that all evaluated models consistently demonstrate the first outcome, effectively leveraging in-context examples; furthermore, performance increases consistently as more shots are used. Motivated by these observations, we seek a more comprehensive understanding of how models perform off-by-one addition, and in particular, the +1 step of the task. To this end, we employ mechanistic interpretability and path patching techniques (Wang et al., 2023), which enables us to trace the model's output logits to a specific set of attention heads and their interconnections responsible for +1 behavior.

Our analysis with `Gemma-2 (9B)` (Gemma Team, 2024) reveals that the model's computation of +1 is mainly governed by three groups of attention heads. Notably, two of these groups and their connections resemble the structure of the induction head mechanism described in prior work (Olsson et al., 2022)[2]. This observation leads to our hypothesis of a *function induction* mechanism—a notable generalization of the induction head mechanism that transcends *token-level* pattern matching to operate at the *function-level*. Our analysis also reveals that the +1 function is transmitted along six (or more) paths in the model's computation graph; in each path, an attention head writes a distinct fraction of the function, whose aggregate effect yields the complete +1 function.

We further validate the universality of our findings across models and tasks (Olah et al., 2020; Merullo et al., 2024). Regarding models, we repeat our analysis on `Mistral-v0.1 (7B)` (Jiang et al., 2023), `Llama-2 (7B)` (Touvron et al., 2023) and `Llama-3 (8B)` (Touvron et al., 2023), confirming the existence of the function induction mechanism, though in slightly varied forms. Regarding tasks, we extend our analysis with four task pairs—off-by-k addition, shifted multiple-choice QA, Caesar Cipher, and base-8 addition—designed to replace sub-steps in off-by-one addition with substantially different operations. We demonstrate the reuse of the same mechanism in these task pairs.

Overall, our results advance our understanding of important language model capabilities such as in-context learning and latent multi-step reasoning. They highlight the flexible and composable nature of the function induction mechanism we have characterized, and provide substantive insights into how models may generalize when encountering novel task variations.

2 LMs Learn Off-by-One Addition in Context

Off-by-one addition is a synthetic, counterfactual task involving two steps. The first step is standard addition, and the second, unexpected step is a +1 function. In this work, we are interested in whether and how the model can perform this task with in-context learning. We provide concrete 4-shot examples of standard addition and off-by-one addition in Table 1. In this section, we first evaluate contemporary language models on this task and describe our observations.

Base Task	Standard Addition	4+3=7\n3+2=5\n6+0=6\n3+3=6\n1+0= **1**
Contrast Task	Off-by-One Addition	4+3=8\n3+2=6\n6+0=7\n3+3=7\n1+0= **2**

Table 1: **Example Prompt of Standard and Off-by-One Addition.** Red is used to mark the base prompt and answer. Orange is used to mark the contrast prompt and answer.

Data. To create the evaluation data, we randomly sample 100 test cases, each with 32 in-context examples ($a_i + b_i = c_i$) and one test example ($a_{test} + b_{test} = c_{test}$). We sample a, b, c from the range of [0,999], and restrict that for all i, $c_{test} \neq c_i$. This is to make sure these test cases evaluate models on inducing +1 function, instead of copying and pasting the answer token (c_{test}) from the previous context (c_i).

Models. We evaluate six recent LMs on this task: `Llama-2 (7B)` (Touvron et al., 2023), `Mistral-v0.1 (7B)` (Jiang et al., 2023), `Gemma-2 (9B)` (Gemma Team et al., 2024), `Qwen-2.5 (7B)` (Yang et al., 2024a), `Llama-3 (8B)` (Grattafiori et al., 2024) and `Phi-4 (14B)` (Abdin et al., 2024). These models were developed by different organizations, employ different number tokenization methods, and were released in different years, thereby providing a diverse and representative sample. Please refer to Table 4 for details of these models.

[2]Induction heads (Olsson et al., 2022) facilitate a language model's token copying behavior in sequences like `[A][B]...[A]` → `[B]` by directly copying *token* `[B]` from the context. Our work aims to explain a more abstract, *function*-level behavior—how models induce the function $f(x) = x + 1$ from sequences like `[A]` f`([B])` ... `[C]` → f`([D])` (*e.g.*, 1+1 = 3 ... 3+3 = 7). See Appendix B for further details.

Evaluation Results. In Fig. 1, we report the accuracy when different numbers of in-context examples are used. All evaluated models exhibit non-trivial performance on this task, demonstrating that this behavior is pervasive. Additionally, performance always improves as the number of shots increases, indicating effective utilization of the in-context examples. Notably, more recent models like `Llama-3 (8B)` and `Phi-4 (14B)` achieve the strongest performance, with near perfect results in the 8-shot experiments. More details of our evaluation (*e.g.*, reporting accuracy on standard addition, using a smaller number range like [0,9], or removing the restriction of $c_{test} \neq c_i$) are deferred to §C.

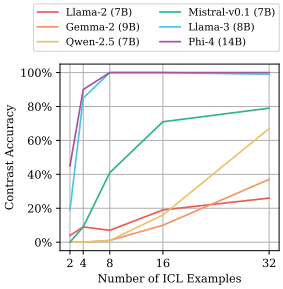

Figure 1: **In-context Learning Performance of Off-by-One Addition.**

3 Interpreting the Off-by-One Addition Algorithm

Off-by-one addition is likely an unseen task to these language models and represents a novel challenge, yet as Fig. 1 shows, they effectively induced the +1 operation with in-context learning.

Intrigued by these observations, we aim to interpret the model's internal computation behind this behavior. §3.1 provides a brief overview of mechanistic interpretability and path patching, a line of methods that we find highly suited to our investigation. We further formalize our notation in this section. In §3.2 we describe our circuit discovery process and findings.

We choose `Gemma-2 (9B)` as the default model based on our preliminary experiments (§C), and use "1+1=3\n2+2=5\n3+3=?" as a running example in the following. Unless specified otherwise, all experiments below use 100 off-by-one addition test cases using numbers in the range of [0,9].[3]

3.1 Background: Mechanistic Interpretability and Path Patching

Mechanistic interpretability is a subfield of interpretability that aims to reverse-engineer model computations and establish "correspondence between model computation and human-understandable concepts." (Wang et al., 2023) A transformer-based language model can be viewed as a computation graph M, where components like attention heads and MLP layers serve as nodes, and their connections as edges. We use $M(y|x)$ to denote the logit of token y when using x as the input prompt. A circuit C is a subgraph of M that is responsible for a certain behavior. In our study, the behavior of interest is the induction and application of the +1 function in off-by-one addition.

The specific method we rely on is path patching (Wang et al., 2023), which is built on activation patching (Meng et al., 2022) and causal mediation (Vig et al., 2020) methods from prior work. In the past, such technique has supported interpretability findings on a wide range of model behaviors (Hanna et al., 2023; Stolfo et al., 2023; Prakash et al., 2024b; Li et al., 2025).

Extending path patching to our case, we first run forward passes on both the base prompt x_{base} (1+1=2\n2+2=4\n3+3=) and contrast prompt x_{cont} (1+1=3\n2+2=5\n3+3=), to obtain the logits $M(.|x_{base})$ and $M(.|x_{cont})$. We will then (1) replace part of the activations in $M(.|x_{cont})$ with the corresponding activations in $M(.|x_{base})$; (2) let the replaced activations propagate to designated target nodes (*e.g.*, output logits, query of a specific head) in the graph; (3) replace the activations of the target nodes in $M(.|x_{cont})$ with the activations obtained in (2). The computation graph after such replacement is denoted as M'. If such a replacement alters the model's output of "3+3=**7**" back to "3+3=**6**", we would believe that the part has contributed to the computation of the +1 function.

To simplify the notation, we define $F(C, x)$ as the logit difference between y_{base} (**6**) and y_{cont} (**7**) when prompted with x and using the circuit C while knocking out nodes outside C in the computation graph, *i.e.*, $F(C, x) = C(y_{base}|x) - C(y_{cont}|x)$. Following Wang et al. (2023), we quantify the effect of a replacement by first computing $F(M', x_{cont})$, and then normalize it by the logit difference before intervention, *i.e.*, $r = \frac{F(M',x_{cont})-F(M,x_{cont})}{F(M,x_{cont})-F(M,x_{base})}$. See §D.1 for its expansion and explanations. The resulting ratio r, which we refer to as relative logit difference, will typically fall in the range

[3]To accommodate our computational resources, circuit discovery experiments (§3.2) were conducted with 4 shots (accuracy=33%), while circuit evaluation experiments (§4) were performed with 16 shots (accuracy=86%).

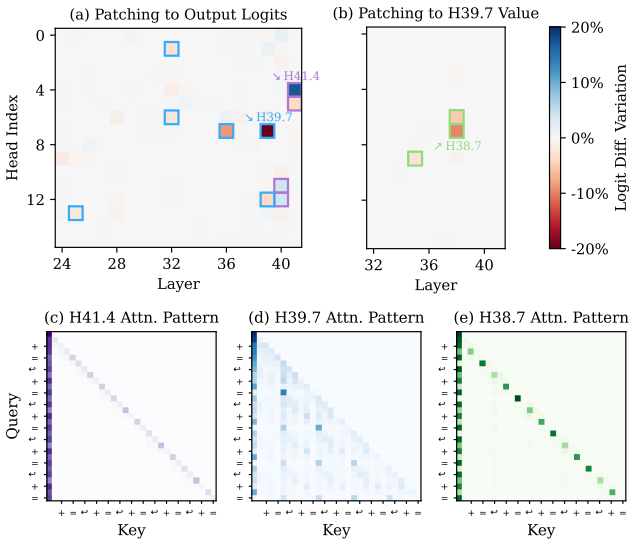

Figure 2: **Circuit Discovery with `Gemma-2 (9B)`. Top: Patching Results on Selected Target Nodes.**
(a) We identify Group 1 heads and Group 2 heads that directly influence the output logits.
(b) We identify Group 3 heads that write to the value of H39.7.
Bottom: Attention Pattern of Selected Heads. We use 4 ICL examples in the format of "a+b=c\n".
(c) Group 1 heads mainly attend to the current token and <bos>.
(d) Group 2 heads attend to the answer tokens (c_i) of previous ICL examples at the position of "=".
(e) Group 3 heads attend to the preceding "=" at the position of c_i.

of [-100%, 0%], with -100% representing the model favors y_{base} (*i.e.*, the model losts its ability on off-by-one addition after replacement), and 0% representing the model favors y_{cont}.

3.2 Circuit Discovery

Patching to the Output Logits. Our investigation begins by setting the output logits as the target node, effectively asking "which attention heads directly influence the model output?" The results, visualized in Fig. 2(a), highlight 10 attention heads with a relative logit difference $|r| > 2\%$.

We further investigate the attention pattern of the highlighted heads and categorized them into two groups. Group 1 heads appear exclusively in the last two layers of the model, and mainly attend to the current token and the <bos> token at each position (Fig. 2(c)). Group 2 heads present periodical patterns consistent with the ICL examples in the prompt (Fig. 2(d)). Specifically, at the position of the last "=" token, where the model is expected to generate the answer as the next token, these attention heads will attend to the answer tokens (c_i) in previous ICL examples ($a_i + b_i = c_i$).

We additionally conduct path patching using the value of Group 1 heads as the target node, revealing that Group 2 heads also write to the value of Group 1 heads which then indirectly influence the final output logits. Combining these findings, we hypothesize that Group 1 heads are responsible for finalizing and aggregating information, while Group 2 heads are responsible for carrying the +1 function from the in-context examples to the test example.

Patching to the Value of Group 2 Heads. To further trace down the origin of the +1 function, we set the value of each head in Group 2 as the target node for path patching. For example, H39.7 (Head 7 in Layer 39) is a representative head in Group 2 with a relative logit difference r of -27% when patching to the final output. When setting H39.7's value as the target node and performing path patching, three heads are highlighted (Fig. 2(b)) and all of these heads follow the pattern of attending to the previous token at certain positions (Fig. 2(e)). In particular, at the answer token c_i in each in-context example, these head attend to the "=" token immediately before c_i. We repeat this procedure for remaining heads in Group 2 and identify more attention heads with the previous-token attending behavior. We collectively refer to them as Group 3 heads.

Our subsequent path patching attempts do not uncover any new attention heads leading to significant logit differences, thus we conclude the algorithm at this point.

The Function Induction Hypothesis. Fig. 3 provides an overview of the circuit we identified, illustrating the connections of the three head groups and highlighting the token positions they operate on. The comprehensive list of heads in each group can be found in §D.2.1 and Fig. 21(b).

We find it particularly intriguing that the structure of the circuit, in particular Group 2 and Group 3, resembles the structure of induction heads (Olsson et al., 2022), a known mechanism responsible for language model's copy-paste behavior. In the induction head mechanism, a previous token head

"copies information from the previous token to the next token", and an induction head "uses that information to find tokens preceded by the present token." (Olsson et al., 2022) We provide an illustration for the original induction head mechanism in §B.

We hypothesize that the circuit we identify generalizes this known mechanism from the token-level to the function-level. Based on this intuition, the three groups of attention heads will cooperate as follows:

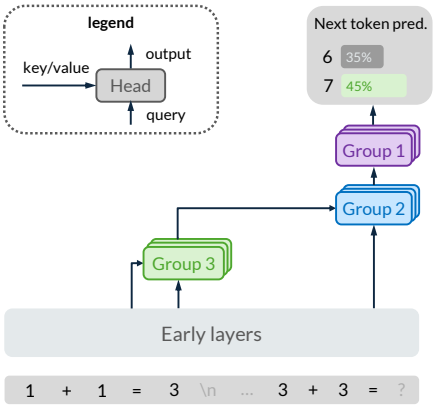

Figure 3: **Overview of the Identified Circuit.**

- Within an ICL example, at the "=" token (*e.g.*, "1+1="), the model initially drafts its answer via early-layer computations (*e.g.*, "2"), and anticipates to generate it as the subsequent token. However, at the answer token position c_i, the model encounters an unexpected answer (*e.g.*, "3"). Consequently, heads in Group 3 register this discrepancy at the position of c_i. Given their previous-token attending behavior, we name heads in Group 3 as previous token (PT) heads.
- In the test example portion of the prompt (*e.g.*, "3+3="), Group 2 heads retrieve the information registered by Group 3 heads at the "=" token, and subsequently writes out the +1 function. We name Group 2 heads as function induction (FI) heads as their operation resembles that of standard induction heads but applies to arithmetic functions rather than tokens.
- Lastly, we refer to Group 1 heads as consolidation heads, hypothesizing their role in finalizing the next-token output by synthesizing information from various sources.

4 Circuit Validation and Analysis

Previously, we constructed the function induction hypothesis based on our path patching results and its structural similarity to that of the induction heads mechanism. In this section, we dive deeper into the identified circuit, aiming to provide a more granular understanding.

Initial Validation: Ablating FI Heads. We begin our investigation with head ablation, a common technique to validate a head's involvement in a specific model behavior (Halawi et al., 2023; Wu et al., 2025). Here, we focus on FI heads and "ablate" a head by replacing its output in the forward pass on x_{cont} with the corresponding head output in the forward pass on x_{base}. As shown in Fig. 4(a), the complete, unablated model achieved an accuracy of 86% on 16-shot off-by-one addition. Upon ablating the six FI heads, the model's behavior switched back to standard addition, resulting in 100% accuracy on standard addition and 0% on off-by-one addition. For a controlled comparison, we also ablated six randomly selected heads; these showed minimal influence on either the base or contrast accuracy. This set of results provides preliminary evidence that the six FI heads are necessary in off-by-one addition.

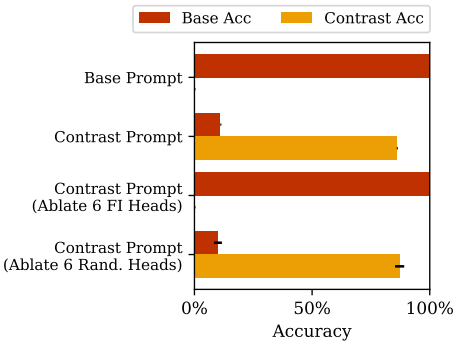

Figure 4: **Head Ablation Results.**

Further Validation: Measuring the Causal Effect of FI Heads. In our hypothesis, FI heads are responsible for writing the +1 function to the residual stream at the "=" token. This behavior is highly relevant to recent work (Todd et al., 2024; Hendel et al., 2023) which indicates that a small number of attention heads (*i.e.*, function vector heads) effectively transport task representations (*i.e.*, function vectors) in in-context learning. The FI heads we identified align with this description, and moreover, uncover a novel instantiation of the mechanism that operates within multi-step tasks.

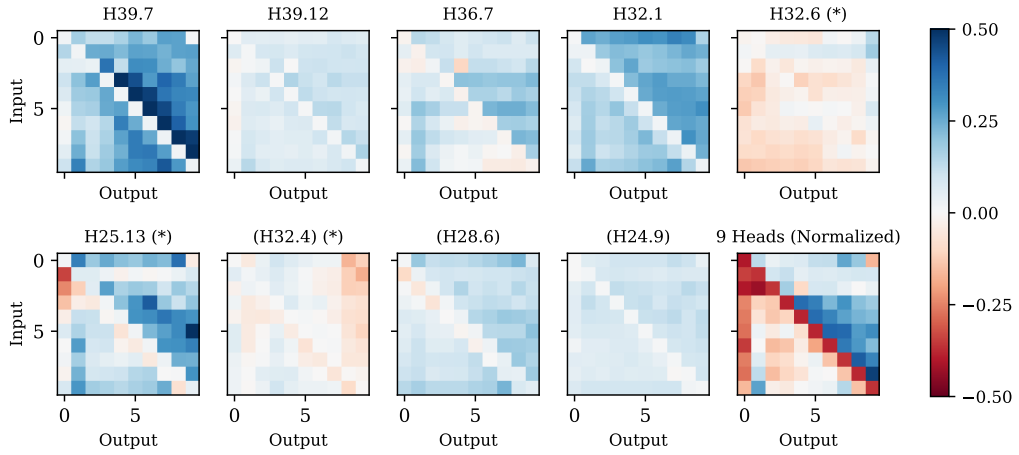

Figure 5: **Individual and Overall Effect of Identified FI Heads.** Each head writes out different information, which aggregates to implement the function of $f(x) = x + 1$ (bottom-right panel). (*) Effects of H32.6, H25.13, and H32.4 are rescaled to [-0.15, 0.15] to make the patterns more readable.

The notion of function vectors inspires us to further validate the role of FI heads through their causal effect on a naive prompt x_{naive}, *e.g.*, "2=2\n3=?", for which the model is expected to assign a high probability to "3". If a FI head indeed writes out the +1 function, adding its output to the residual stream at the final "=" token should cause the model to increase its probability of generating "4".

Concretely, we construct the naive prompt "{x-1}={x-1}\n{x}=?" for $x \in [0, 9]$, and track the model's logits for tokens $[0, 9]$ both before and after adding the FI head output to the residual stream at the corresponding layer. This leads to a 10×10 heatmap, where the value at cell (x_{input}, y_{output}) represents the change in logits for token y when the function vector is added.

In Fig. 5, we present these heatmaps for each of the six FI heads identified in §3.2. We include three additional heads (H32.4, H28.6, H24.9) that, while showing modest effects ($1\% < |r| < 2\%$) in §3.2, contribute meaningfully to the +1 function as revealed by this analysis. We find that FI heads work collaboratively—each of them contributes a distinct piece to the overall +1 function. For example, with an input x, H39.7 promotes $x + 1$, H28.6 suppress $x - 1$, H32.1 promotes digits greater than x, H24.9 suppresses x. When the outputs of these nine heads are added to the final residual stream altogether, their combined effect implements the +1 function, as depicted in the last panel of Fig. 5.

Universality of Function Induction. To investigate the universality of our findings across models, we repeat the path patching experiments with `Llama-3 (8B)`, `Llama-2 (7B)`, and `Mistral-v0.1 (7B)`. We identified all three groups of heads across these models, except that the two consolidation heads identified in `Mistral-v0.1` display weaker and less consistent signals. Still, these observations provide promising evidence that the function induction mechanism is general and consistently emerges across various language models. See §D.2 for more details.

FI Heads (Ours) and FV Heads (Todd et al., 2024) are Two Disjoint Sets of Heads. While our analysis demonstrates that FI heads transport task representations similarly to the FV heads described in prior work, a direct comparison with `Llama 2 (7B)` reveals important distinctions. Todd et al. (2024) reported that FV heads appear in early-middle layers of the model (before layer 20), whereas our FI heads are located in late layers of the model (layer 29-31). There is no overlap between the two sets of heads, suggesting that our work presents a distinct, previously undocumented finding. We hypothesize that FI heads can be seen as an instantiation of the broader FV head mechanism, but are only triggered in multi-step tasks where late layers are used to perform the late steps. See §D.2.4 for the full list of FI/FV heads and §6 for related discussions.

Additional Analysis. Due to space limits, we defer various supporting evidence to the appendix. We conduct a rigorous evaluation of our circuit using the *faithfulness*, *completeness*, and *minimality* criteria introduced in Wang et al. (2023). Our circuit mostly satisfies these criteria, and we discuss the results in §E. We deliberately focus on FI heads in §4 given the interesting insights from these results. We provide further validation and analysis of consolidation heads and previous token heads in §F.

5 Task Generalization with Function Induction

Our investigation so far suggests that function induction is the key mechanism enabling the model to generalize from standard addition and manage the unexpected +1 step in off-by-one addition. Given the importance of task generalization for capable AI systems, we aim to explore the broader usage of this mechanism. In this section, we investigate the role of function induction in a range of synthetic and algorithmic tasks. Specifically, §5.1 introduces the four task pairs examined, and §5.2 presents the overall findings and additional analyses for two of these pairs.

5.1 Tasks

(a) Off-by-k Addition		(c) Caeser Cipher	
Standard	4+3=7\n3+2=5\n6+0=6\n3+3=6\n1+0= **1**	ROT-0	c -> c\nx -> x\ne -> e\nt -> t\nq -> **q**
Off-by-Two	4+3=9\n3+2=7\n6+0=8\n3+3=8\n1+0= **3**	ROT-2	c -> e\nx -> z\ne -> g\nt -> v\nq -> **s**
(b) Shifted MMLU		**(d) Base-k Addition**	
Standard	[...]\nAnswer: (B)\n[...]\nAnswer: **(A)**	Base-10	25+16=41\n60+16=76\n13+35=48\n52+17= **69**
Shift-by-One	[...]\nAnswer: (C)\n[...]\nAnswer: **(B)**	Base-8	25+16=43\n60+16=76\n13+35=50\n52+17= **71**

Table 2: **Task Pairs Used in Task Generalization Experiments.** Red is used to mark the base prompt and answer. Orange is used to mark the contrast prompt and answer.

(a) Off-by-k Addition. One extension of off-by-one addition is changing the offset to other values. Here, we consider offsets $k \in \{-2, -1, 2\}$. We use $k = 2$ as a representative case to be reported in the main paper. Results and analysis on the other offsets are deferred to §G.

(b) Shifted Multiple-choice QA. We consider going beyond arithmetic tasks and replace steps in off-by-one addition with substantively different steps. The base task is chosen to be multiple-choice QA questions on selected subjects of the MMLU dataset (Hendrycks et al., 2021). The contrast task is created with an additional step to shift the answer choice letter by one letter, *e.g.*, A→B, B→C.

(c) Caesar Cipher. One realistic task that leverages shifting functions is Caesar Cipher. During encoding, a letter is replaced by the corresponding letter a fixed number of positions down the alphabet (Wikipedia contributors, 2025). This task is also commonly used to evaluate a language model's reasoning capabilities (Prabhakar et al., 2024). Here we consider single-character Ceaser Cipher with different offsets $k \in \{-12, -11, \ldots, 0, \ldots, 12, 13\}$. We use $k = 0$ as the base task, and $k = 2$ as the representative contrast task.

(d) Base-k Addition. Lastly, we consider the task of base-k addition, which was used by Wu et al. (2024) to assess the a model's memorization versus generalization. Prior work (Ye et al., 2024) suggests that LMs may formulate a shortcut solution for base-8 addition by interpreting it as "adding 22 to the sum" from in-context examples; our interpretability analysis helps further investigate this observation. We consider two digit base-10 addition as the base task, and base-k addition as the contrast task, with $k \in \{6, 7, 8, 9\}$. We use $k = 8$ as a representative case in the main paper.

5.2 Results and Analysis

FI heads are reused in a wider range of tasks. Using the four task pairs introduced above, we examine the role of the function induction mechanism we discover with head ablation experiments, similar to the one done in Fig. 4. We run forward passes on both the base task and the contrast task. We then replace the FI heads outputs in $M(.|x_{cont})$ forward pass with the corresponding head outputs in the $M(.|x_{base})$ forward pass.

We report results of the representative cases in Fig. 6. In all four task pairs, we first see a non-trivial performance on the contrast task, indicating effective generalization. Upon ablating the six FI heads, we observe a consistent trend: the model's contrast accuracy substantially decreases; the base accuracy increases and often returns to a level comparable to that achieved with the base prompt.

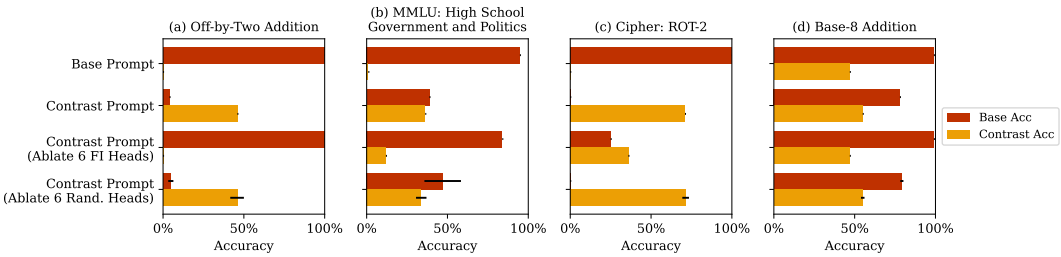

Figure 6: **Task Generalization with FI Heads.** In (d), base-8 addition has non-zero accuracy with the base-10 prompt, because in these test cases the base-10 answers happen to be correct in base-8.

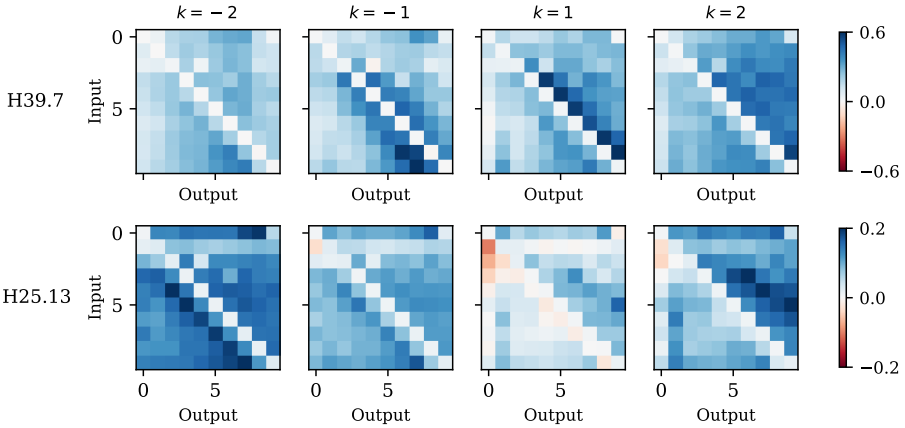

Figure 7: **Effect of Two FI heads When Using Different Offsets in Off-by-k Addition.**

These findings suggest that the mechanism identified with off-by-one addition is largely reused in these task pairs, which share a similar underlying structure but also represents substantially different sub-steps. This strongly demonstrates the mechanism's flexibility and composability.

We also observe that in (b) Shifted MMLU and (c) Caesar Cipher, the model has non-zero contrast accuracies when the FI heads are ablated. This implies that the six FI heads we found with off-by-one addition are useful, but not complete for these task pairs. See §G for additional discussion.

Function vector analysis with off-by-k addition. We revisit the function vector style analysis done in Fig. 5, but this time considering different offsets $k \in \{-2, -1, 1, 2\}$. Results on two representative heads (H39.7 and H25.13) are shown in Fig. 7, with other heads deferred to Fig. 23-25.

We find that the effect of FI heads varies meaningfully with the offset k, demonstrating their generality and consistency with the hypothesized functionality. For the two selected heads in Fig. 7, we find that each of them has their own "specialty." For example, the heatmap for H25.13 suggests its primary responsibility for writing out ± 2 functions. While its effect is stronger when the offset $k = \pm 2$, it still contributes in the case of $k = \pm 1$ by suppressing the original output x.

Models struggle in base-8 addition due to under- or over-generalization. It may sound unintuitive why the induction mechanism specialized in shifting functions could facilitate base-8 addition. One possible explanation is that the model initially performs standard base-10 addition with early layers, and apply minor adjustments when necessary. This adjustment step is possibly handled by the function induction mechanism in late layers.

Following this intuition, we propose one possible algorithm for two-digit base-8 addition in Listing 1. No adjustment is needed when there is no carrying over from the unit digit (Case 1), *e.g.*, $60+16 = 76$ is correct in both base-8 and base-10. When carry-over occurs, two separate cases needs to be considered. In Case 2, both the unit and the eight's place digit require adjustment, *e.g.*, $13_8 + 35_8 = 50_8$ and $13_{10} + 35_{10} = 48_{10}$, so both 4 and 8 in 48_{10} need to be adjusted. In Case 3, only the unit digit needs adjustment, *e.g.*, $25_8 + 16_8 = 43_8$ and $25_{10} + 16_{10} = 41_{10}$.

We randomly sample 100 32-shot prompts for each of these three cases, and track the model's behavior on the unit and eight's place digit. We report the results in Table 3. In Case 1, digits are adjusted unnecessarily in 7% (=6%+1%) of instances, suggesting over-generalization. Conversely, in Case 2 and 3, digits were not adjusted as expected in 84% (=68%+16%) and 83% of instances, suggesting under-generalization. Overall, this evidence suggests that while the model can induce simple functions like +2 to some extent, it struggles with more complex situations where +2 should be only be triggered under certain *conditions*. Alternatively, if the induction of these conditions is viewed as an additional step in multi-step reasoning, the model we investigate may not yet be capable of two-step induction in a three-step task, thereby limiting their performance in base-8 addition.

```python
def base8addition(a, b):
    # (1) perform base-10 addition
    c = base10addition(a, b) # case 1
    # (2) apply adjustments
    if 8 <= a[0] + b[0] < 10: # case 2
        c[0] = (c[0] + 2) % 10
        c[1] = c[1] + 1
    elif a[0] + b[0] >= 10: # case 3
        c[0] = c[0] + 2
    return c
```

Listing 1: **One possible algorithm for two-digit base-8 addition.** This algorithm divides all scenarios into three cases. `c[0]` represents the unit digit and `c[1]` represents the tens/eights digit in a two-digit number `c`.

Case	Full Model				Ablate FI Heads
	Neither	`c[0]`	`c[1]`	Both	Neither
Case 1	93	6	1	0	100
Case 2	68	0	16	16	100
Case 3	83	14	0	0	100

Table 3: **Error analysis for two-digit base-8 addition.** We use 100 examples for each case specified in Listing 1. The correct behavior is marked in green. "Neither" suggests the number of times that neither `c[0]` or `c[1]` is adjusted, which is anticipated in Case 1. "`c[0]`" suggests that *only* `c[0]` is adjusted. "Both" suggests both digits are adjusted.

6 Related Works

Mechanistic Interpretability. The field of mechanistic interpretability aims to reverse-engineer complex neural networks into human-understandable algorithms (Bereska & Gavves, 2024; Sharkey et al., 2025), enhancing our understanding of a wide range of model behaviors, including in-context learning (Olsson et al., 2022), long-context retrieval (Wu et al., 2025), and chain-of-thought reasoning (Cabannes et al., 2024). A common methodology involves analyzing their computation graphs of a specific task, as exemplified by studies on indirect object identification (Wang et al., 2023), "greater than" operation (Hanna et al., 2023), and entity tracking (Prakash et al., 2024a). Following this, our work begins with the off-by-one addition task, and showcases the broader applicability of our findings with various task pairs.

Function Vectors in LMs. Recent work has characterized in-context learning in language models as the compression of in-context examples into a single task or function vector, which is subsequently transported to the test example to trigger the model to apply the function (Todd et al., 2024; Hendel et al., 2023; Yin & Steinhardt, 2025). These studies present strong evidence pertaining to *single-step*, *mapping-style* tasks like country-to-capital and English-French translation. Our work is inspired by this line of research, yet with two key differences: (1) We focus on off-by-one addition, a *multi-step arithmetic* task, where the learning of the second step depends on the results of the preceding step. (2) We provide a finer-grained interpretation on how function vectors, sent out by different attention heads, vary in content but collaborate to form a complete function. In concurrent work, this latter aspect was also explored by Hu et al. (2025), who investigate the task of add-k (*i.e.*, "5→8, 1→4, 2→?") using subspace decomposition.

Latent Multi-step Reasoning and Structural Compositionality in LMs. Various studies investigate whether and how models perform latent multi-step reasoning, typically via multi-hop factoid QA tasks (Yang et al., 2024b; Wang et al., 2024). Our work demonstrates that LMs can dynamically infer the second step in a two-step problem from in-context examples, a process representing a novel, flexible and composable form of latent multi-step reasoning. More broadly, our findings are relevant to research investigating structural compositionality (Lepori et al., 2023) (*i.e.*, breaking down complex tasks into subroutines) in language models.

7 Conclusion

In this work, we present an interpretability study on the off-by-one addition task, with the broader goal of investigating how language models handle unseen tasks using in-context learning. Our analysis led to the discovery of a function induction mechanism, which handles the "twists" involved in generalizing from seen to unseen tasks. This discovery extends and generalizes previous interpretability findings on induction heads and function vectors. We further show this mechanism is broadly reused beyond off-by-one addition, notably in realistic algorithmic tasks like Caesar Cipher and base-8 addition. Collectively, these observations deepen our understanding of what language models are capable of with in-context learning and multi-step reasoning, and how models generalize to novel tasks and situations. Moreover, our work provides compelling evidence that language models may develop composable and general mechanisms for handling ever-changing task variations, suggesting one possible pathway toward explaining and perhaps further enhancing model capabilities.

Acknowledgment

We thank anonymous reviewers who provided valuable feedback on our work. We thank Xisen Jin, Ting-Yun Chang, Lorena Yan, Yuqing Yang, Deqing Fu, Ollie Liu, Daniel Firebanks-Quevedo, Johnny Wei, as well as members of USC INK Lab and Allegro Lab for insightful discussions. QY and XR were supported in part by the Office of the Director of National Intelligence (ODNI), Intelligence Advanced Research Projects Activity (IARPA), via the HIATUS Program contract #2022-22072200006, the Defense Advanced Research Projects Agency with award HR00112220046, and NSF IIS 2048211. QY was also supported by a USC Annenberg Fellowship. RJ was supported in part by the National Science Foundation under Grant No. IIS-2403436. Any opinions, findings, and conclusions or recommendations expressed in this material are those of the author(s) and do not necessarily reflect the views of the National Science Foundation.

References

Marah Abdin, Jyoti Aneja, Harkirat Behl, Sébastien Bubeck, Ronen Eldan, Suriya Gunasekar, Michael Harrison, Russell J. Hewett, Mojan Javaheripi, Piero Kauffmann, James R. Lee, Yin Tat Lee, Yuanzhi Li, Weishung Liu, Caio C. T. Mendes, Anh Nguyen, Eric Price, Gustavo de Rosa, Olli Saarikivi, Adil Salim, Shital Shah, Xin Wang, Rachel Ward, Yue Wu, Dingli Yu, Cyril Zhang, and Yi Zhang. Phi-4 technical report, 2024. URL https://arxiv.org/abs/2412.08905.

Leonard Bereska and Stratis Gavves. Mechanistic interpretability for AI safety - a review. *Transactions on Machine Learning Research*, 2024. ISSN 2835-8856. URL https://openreview.net/forum?id=ePUVetPKu6. Survey Certification, Expert Certification.

Tom Brown, Benjamin Mann, Nick Ryder, Melanie Subbiah, Jared D Kaplan, Prafulla Dhariwal, Arvind Neelakantan, Pranav Shyam, Girish Sastry, Amanda Askell, Sandhini Agarwal, Ariel Herbert-Voss, Gretchen Krueger, Tom Henighan, Rewon Child, Aditya Ramesh, Daniel Ziegler, Jeffrey Wu, Clemens Winter, Chris Hesse, Mark Chen, Eric Sigler, Mateusz Litwin, Scott Gray, Benjamin Chess, Jack Clark, Christopher Berner, Sam McCandlish, Alec Radford, Ilya Sutskever, and Dario Amodei. Language models are few-shot learners. In H. Larochelle, M. Ranzato, R. Hadsell, M.F. Balcan, and H. Lin (eds.), *Advances in Neural Information Processing Systems*, volume 33, pp. 1877–1901. Curran Associates, Inc., 2020. URL https://proceedings.neurips.cc/paper_files/paper/2020/file/1457c0d6bfcb4967418bfb8ac142f64a-Paper.pdf.

Vivien Cabannes, Charles Arnal, Wassim Bouaziz, Alice Yang, Francois Charton, and Julia Kempe. Iteration head: A mechanistic study of chain-of-thought. In A. Globerson, L. Mackey, D. Belgrave, A. Fan, U. Paquet, J. Tomczak, and C. Zhang (eds.), *Advances in Neural Information Processing Systems*, volume 37, pp. 109101–109122. Curran Associates, Inc., 2024. URL https://proceedings.neurips.cc/paper_files/paper/2024/file/c50f8180ef34060ec59b75d6e1220f7a-Paper-Conference.pdf.

Yanda Chen, Ruiqi Zhong, Sheng Zha, George Karypis, and He He. Meta-learning via language model in-context tuning. In Smaranda Muresan, Preslav Nakov, and Aline Villavicencio (eds.), *Proceedings of the 60th Annual Meeting of the Association for Computational Linguistics (Volume 1:*

Long Papers), pp. 719–730, Dublin, Ireland, May 2022. Association for Computational Linguistics. doi: 10.18653/v1/2022.acl-long.53. URL https://aclanthology.org/2022.acl-long.53/.

Nelson Elhage, Neel Nanda, Catherine Olsson, Tom Henighan, Nicholas Joseph, Ben Mann, Amanda Askell, Yuntao Bai, Anna Chen, Tom Conerly, et al. A mathematical framework for transformer circuits. *Transformer Circuits Thread*, 1(1):12, 2021.

Javier Ferrando and Elena Voita. Information flow routes: Automatically interpreting language models at scale. *Arxiv*, 2024. URL https://arxiv.org/abs/2403.00824.

Gemma Team, Morgane Riviere, Shreya Pathak, Pier Giuseppe Sessa, Cassidy Hardin, Surya Bhupatiraju, Léonard Hussenot, Thomas Mesnard, Bobak Shahriari, Alexandre Ramé, et al. Gemma 2: Improving open language models at a practical size. *arXiv preprint arXiv:2408.00118*, 2024.

Aaron Grattafiori, Abhimanyu Dubey, Abhinav Jauhri, Abhinav Pandey, Abhishek Kadian, Ahmad Al-Dahle, Aiesha Letman, Akhil Mathur, Alan Schelten, Alex Vaughan, et al. The llama 3 herd of models. *arXiv preprint arXiv:2407.21783*, 2024.

Danny Halawi, Jean-Stanislas Denain, and Jacob Steinhardt. Overthinking the truth: Understanding how language models process false demonstrations, 2023. URL https://openreview.net/forum?id=em4xg1Gvxa.

Michael Hanna, Ollie Liu, and Alexandre Variengien. How does GPT-2 compute greater-than?: Interpreting mathematical abilities in a pre-trained language model. In *Thirty-seventh Conference on Neural Information Processing Systems*, 2023. URL https://openreview.net/forum?id=p4PckNQR8k.

Roee Hendel, Mor Geva, and Amir Globerson. In-context learning creates task vectors. In Houda Bouamor, Juan Pino, and Kalika Bali (eds.), *Findings of the Association for Computational Linguistics: EMNLP 2023*, pp. 9318–9333, Singapore, December 2023. Association for Computational Linguistics. doi: 10.18653/v1/2023.findings-emnlp.624. URL https://aclanthology.org/2023.findings-emnlp.624/.

Dan Hendrycks, Collin Burns, Steven Basart, Andy Zou, Mantas Mazeika, Dawn Song, and Jacob Steinhardt. Measuring massive multitask language understanding. In *International Conference on Learning Representations*, 2021. URL https://openreview.net/forum?id=d7KBjmI3GmQ.

Xinyan Hu, Kayo Yin, Michael I. Jordan, Jacob Steinhardt, and Lijie Chen. Understanding in-context learning of addition via activation subspaces, 2025. URL https://arxiv.org/abs/2505.05145.

Samyak Jain, Robert Kirk, Ekdeep Singh Lubana, Robert P. Dick, Hidenori Tanaka, Tim Rocktäschel, Edward Grefenstette, and David Krueger. Mechanistically analyzing the effects of fine-tuning on procedurally defined tasks. In *The Twelfth International Conference on Learning Representations*, 2024. URL https://openreview.net/forum?id=A0HKeKl4Nl.

Albert Q. Jiang, Alexandre Sablayrolles, Arthur Mensch, Chris Bamford, Devendra Singh Chaplot, Diego de las Casas, Florian Bressand, Gianna Lengyel, Guillaume Lample, Lucile Saulnier, Lélio Renard Lavaud, Marie-Anne Lachaux, Pierre Stock, Teven Le Scao, Thibaut Lavril, Thomas Wang, Timothée Lacroix, and William El Sayed. Mistral 7b, 2023. URL https://arxiv.org/abs/2310.06825.

Thomas Kwa, Ben West, Joel Becker, Amy Deng, Katharyn Garcia, Max Hasin, Sami Jawhar, Megan Kinniment, Nate Rush, Sydney Von Arx, Ryan Bloom, Thomas Broadley, Haoxing Du, Brian Goodrich, Nikola Jurkovic, Luke Harold Miles, Seraphina Nix, Tao Lin, Neev Parikh, David Rein, Lucas Jun Koba Sato, Hjalmar Wijk, Daniel M. Ziegler, Elizabeth Barnes, and Lawrence Chan. Measuring ai ability to complete long tasks, 2025. URL https://arxiv.org/abs/2503.14499.

Michael Lepori, Thomas Serre, and Ellie Pavlick. Break it down: Evidence for structural compositionality in neural networks. In A. Oh, T. Naumann, A. Globerson, K. Saenko, M. Hardt, and S. Levine (eds.), *Advances in Neural Information Processing Systems*, volume 36, pp. 42623–42660. Curran Associates, Inc., 2023. URL https://proceedings.neurips.cc/paper_files/paper/2023/file/85069585133c4c168c865e65d72e9775-Paper-Conference.pdf.

Belinda Z Li, Zifan Carl Guo, and Jacob Andreas. (how) do language models track state? *arXiv preprint arXiv:2503.02854*, 2025.

Ziqian Lin and Kangwook Lee. Dual operating modes of in-context learning. In *Forty-first International Conference on Machine Learning*, 2024. URL https://openreview.net/forum?id=ElVHUWyL3n.

Xinxi Lyu, Sewon Min, Iz Beltagy, Luke Zettlemoyer, and Hannaneh Hajishirzi. Z-ICL: Zero-shot in-context learning with pseudo-demonstrations. In Anna Rogers, Jordan Boyd-Graber, and Naoaki Okazaki (eds.), *Proceedings of the 61st Annual Meeting of the Association for Computational Linguistics (Volume 1: Long Papers)*, pp. 2304–2317, Toronto, Canada, July 2023. Association for Computational Linguistics. doi: 10.18653/v1/2023.acl-long.129. URL https://aclanthology.org/2023.acl-long.129/.

Kevin Meng, David Bau, Alex Andonian, and Yonatan Belinkov. Locating and editing factual associations in gpt. In S. Koyejo, S. Mohamed, A. Agarwal, D. Belgrave, K. Cho, and A. Oh (eds.), *Advances in Neural Information Processing Systems*, volume 35, pp. 17359–17372. Curran Associates, Inc., 2022. URL https://proceedings.neurips.cc/paper_files/paper/2022/file/6f1d43d5a82a37e89b0665b33bf3a182-Paper-Conference.pdf.

Jack Merullo, Carsten Eickhoff, and Ellie Pavlick. Circuit component reuse across tasks in transformer language models. In *The Twelfth International Conference on Learning Representations*, 2024. URL https://openreview.net/forum?id=fpoAYV6Wsk.

Sewon Min, Mike Lewis, Luke Zettlemoyer, and Hannaneh Hajishirzi. MetaICL: Learning to learn in context. In Marine Carpuat, Marie-Catherine de Marneffe, and Ivan Vladimir Meza Ruiz (eds.), *Proceedings of the 2022 Conference of the North American Chapter of the Association for Computational Linguistics: Human Language Technologies*, pp. 2791–2809, Seattle, United States, July 2022a. Association for Computational Linguistics. doi: 10.18653/v1/2022.naacl-main.201. URL https://aclanthology.org/2022.naacl-main.201/.

Sewon Min, Xinxi Lyu, Ari Holtzman, Mikel Artetxe, Mike Lewis, Hannaneh Hajishirzi, and Luke Zettlemoyer. Rethinking the role of demonstrations: What makes in-context learning work? In Yoav Goldberg, Zornitsa Kozareva, and Yue Zhang (eds.), *Proceedings of the 2022 Conference on Empirical Methods in Natural Language Processing*, pp. 11048–11064, Abu Dhabi, United Arab Emirates, December 2022b. Association for Computational Linguistics. doi: 10.18653/v1/2022.emnlp-main.759. URL https://aclanthology.org/2022.emnlp-main.759/.

Neel Nanda and Joseph Bloom. Transformerlens. https://github.com/TransformerLensOrg/TransformerLens, 2022.

Neel Nanda, Lawrence Chan, Tom Lieberum, Jess Smith, and Jacob Steinhardt. Progress measures for grokking via mechanistic interpretability. In *The Eleventh International Conference on Learning Representations*, 2023. URL https://openreview.net/forum?id=9XFSbDPmdW.

nostalgebraist. interpreting gpt: the logit lens. https://www.lesswrong.com/posts/AcKRB8wDpdaN6v6ru/interpreting-gpt-the-logit-lens, 2020. Accessed: 2025-06-17.

Chris Olah, Nick Cammarata, Ludwig Schubert, Gabriel Goh, Michael Petrov, and Shan Carter. Zoom in: An introduction to circuits. *Distill*, 2020. doi: 10.23915/distill.00024.001. URL https://distill.pub/2020/circuits/zoom-in.

Catherine Olsson, Nelson Elhage, Neel Nanda, Nicholas Joseph, Nova DasSarma, Tom Henighan, Ben Mann, Amanda Askell, Yuntao Bai, Anna Chen, et al. In-context learning and induction heads. *arXiv preprint arXiv:2209.11895*, 2022.

Akshara Prabhakar, Thomas L. Griffiths, and R. Thomas McCoy. Deciphering the factors influencing the efficacy of chain-of-thought: Probability, memorization, and noisy reasoning. In Yaser Al-Onaizan, Mohit Bansal, and Yun-Nung Chen (eds.), *Findings of the Association for Computational Linguistics: EMNLP 2024*, pp. 3710–3724, Miami, Florida, USA, November 2024. Association for Computational Linguistics. doi: 10.18653/v1/2024.findings-emnlp.212. URL https://aclanthology.org/2024.findings-emnlp.212/.

Nikhil Prakash, Tamar Rott Shaham, Tal Haklay, Yonatan Belinkov, and David Bau. Fine-tuning enhances existing mechanisms: A case study on entity tracking. In *Proceedings of the 2024 International Conference on Learning Representations*, 2024a. arXiv:2402.14811.

Nikhil Prakash, Tamar Rott Shaham, Tal Haklay, Yonatan Belinkov, and David Bau. Fine-tuning enhances existing mechanisms: A case study on entity tracking. In *The Twelfth International Conference on Learning Representations*, 2024b. URL https://openreview.net/forum?id=8sKcAWOf2D.

Lee Sharkey, Bilal Chughtai, Joshua Batson, Jack Lindsey, Jeff Wu, Lucius Bushnaq, Nicholas Goldowsky-Dill, Stefan Heimersheim, Alejandro Ortega, Joseph Bloom, Stella Biderman, Adria Garriga-Alonso, Arthur Conmy, Neel Nanda, Jessica Rumbelow, Martin Wattenberg, Nandi Schoots, Joseph Miller, Eric J. Michaud, Stephen Casper, Max Tegmark, William Saunders, David Bau, Eric Todd, Atticus Geiger, Mor Geva, Jesse Hoogland, Daniel Murfet, and Tom McGrath. Open problems in mechanistic interpretability, 2025. URL https://arxiv.org/abs/2501.16496.

Alessandro Stolfo, Yonatan Belinkov, and Mrinmaya Sachan. A mechanistic interpretation of arithmetic reasoning in language models using causal mediation analysis. In Houda Bouamor, Juan Pino, and Kalika Bali (eds.), *Proceedings of the 2023 Conference on Empirical Methods in Natural Language Processing*, pp. 7035–7052, Singapore, December 2023. Association for Computational Linguistics. doi: 10.18653/v1/2023.emnlp-main.435. URL https://aclanthology.org/2023.emnlp-main.435/.

Alex Tamkin, Miles McCain, Kunal Handa, Esin Durmus, Liane Lovitt, Ankur Rathi, Saffron Huang, Alfred Mountfield, Jerry Hong, Stuart Ritchie, Michael Stern, Brian Clarke, Landon Goldberg, Theodore R. Sumers, Jared Mueller, William McEachen, Wes Mitchell, Shan Carter, Jack Clark, Jared Kaplan, and Deep Ganguli. Clio: Privacy-preserving insights into real-world ai use, 2024. URL https://arxiv.org/abs/2412.13678.

Eric Todd, Millicent Li, Arnab Sen Sharma, Aaron Mueller, Byron C Wallace, and David Bau. Function vectors in large language models. In *The Twelfth International Conference on Learning Representations*, 2024. URL https://openreview.net/forum?id=AwyxtyMwaG.

Hugo Touvron, Louis Martin, Kevin Stone, Peter Albert, Amjad Almahairi, Yasmine Babaei, Nikolay Bashlykov, Soumya Batra, Prajjwal Bhargava, Shruti Bhosale, et al. Llama 2: Open foundation and fine-tuned chat models. *arXiv preprint arXiv:2307.09288*, 2023.

Igor Tufanov, Karen Hambardzumyan, Javier Ferrando, and Elena Voita. Lm transparency tool: Interactive tool for analyzing transformer language models. *Arxiv*, 2024. URL https://arxiv.org/abs/2404.07004.

Jesse Vig, Sebastian Gehrmann, Yonatan Belinkov, Sharon Qian, Daniel Nevo, Yaron Singer, and Stuart Shieber. Investigating gender bias in language models using causal mediation analysis. In H. Larochelle, M. Ranzato, R. Hadsell, M.F. Balcan, and H. Lin (eds.), *Advances in Neural Information Processing Systems*, volume 33, pp. 12388–12401. Curran Associates, Inc., 2020. URL https://proceedings.neurips.cc/paper_files/paper/2020/file/92650b2e92217715fe312e6fa7b90d82-Paper.pdf.

Boshi Wang, Xiang Yue, Yu Su, and Huan Sun. Grokking of implicit reasoning in transformers: A mechanistic journey to the edge of generalization. In *The Thirty-eighth Annual Conference on Neural Information Processing Systems*, 2024. URL https://openreview.net/forum?id=D4QgSWxiOb.

Kevin Ro Wang, Alexandre Variengien, Arthur Conmy, Buck Shlegeris, and Jacob Steinhardt. Interpretability in the wild: a circuit for indirect object identification in GPT-2 small. In *The Eleventh International Conference on Learning Representations*, 2023. URL https://openreview.net/forum?id=NpsVSN6o4ul.

Jerry Wei, Jason Wei, Yi Tay, Dustin Tran, Albert Webson, Yifeng Lu, Xinyun Chen, Hanxiao Liu, Da Huang, Denny Zhou, and Tengyu Ma. Larger language models do in-context learning differently, 2024. URL https://openreview.net/forum?id=DRGnEkbiQZ.

Wikipedia contributors. Caesar cipher — Wikipedia, the free encyclopedia, 2025. URL https://en.wikipedia.org/w/index.php?title=Caesar_cipher&oldid=1294051421. [Online; accessed 12-June-2025].

Thomas Wolf, Lysandre Debut, Victor Sanh, Julien Chaumond, Clement Delangue, Anthony Moi, Pierric Cistac, Tim Rault, Remi Louf, Morgan Funtowicz, Joe Davison, Sam Shleifer, Patrick von Platen, Clara Ma, Yacine Jernite, Julien Plu, Canwen Xu, Teven Le Scao, Sylvain Gugger, Mariama Drame, Quentin Lhoest, and Alexander Rush. Transformers: State-of-the-art natural language processing. In Qun Liu and David Schlangen (eds.), *Proceedings of the 2020 Conference on Empirical Methods in Natural Language Processing: System Demonstrations*, pp. 38–45, Online, October 2020. Association for Computational Linguistics. doi: 10.18653/v1/2020.emnlp-demos.6. URL https://aclanthology.org/2020.emnlp-demos.6/.

Wenhao Wu, Yizhong Wang, Guangxuan Xiao, Hao Peng, and Yao Fu. Retrieval head mechanistically explains long-context factuality. In *The Thirteenth International Conference on Learning Representations*, 2025. URL https://openreview.net/forum?id=EytBpUGB1Z.

Zhaofeng Wu, Linlu Qiu, Alexis Ross, Ekin Akyürek, Boyuan Chen, Bailin Wang, Najoung Kim, Jacob Andreas, and Yoon Kim. Reasoning or reciting? exploring the capabilities and limitations of language models through counterfactual tasks. In Kevin Duh, Helena Gomez, and Steven Bethard (eds.), *Proceedings of the 2024 Conference of the North American Chapter of the Association for Computational Linguistics: Human Language Technologies (Volume 1: Long Papers)*, pp. 1819–1862, Mexico City, Mexico, June 2024. Association for Computational Linguistics. doi: 10.18653/v1/2024.naacl-long.102. URL https://aclanthology.org/2024.naacl-long.102/.

An Yang, Baosong Yang, Beichen Zhang, Binyuan Hui, Bo Zheng, Bowen Yu, Chengyuan Li, Dayiheng Liu, Fei Huang, Haoran Wei, et al. Qwen2.5 technical report. *arXiv preprint arXiv:2412.15115*, 2024a.

Sohee Yang, Elena Gribovskaya, Nora Kassner, Mor Geva, and Sebastian Riedel. Do large language models latently perform multi-hop reasoning? In Lun-Wei Ku, Andre Martins, and Vivek Srikumar (eds.), *Proceedings of the 62nd Annual Meeting of the Association for Computational Linguistics (Volume 1: Long Papers)*, pp. 10210–10229, Bangkok, Thailand, August 2024b. Association for Computational Linguistics. doi: 10.18653/v1/2024.acl-long.550. URL https://aclanthology.org/2024.acl-long.550/.

Qinyuan Ye, Mohamed Ahmed, Reid Pryzant, and Fereshte Khani. Prompt engineering a prompt engineer. In Lun-Wei Ku, Andre Martins, and Vivek Srikumar (eds.), *Findings of the Association for Computational Linguistics: ACL 2024*, pp. 355–385, Bangkok, Thailand, August 2024. Association for Computational Linguistics. doi: 10.18653/v1/2024.findings-acl.21. URL https://aclanthology.org/2024.findings-acl.21/.

Kayo Yin and Jacob Steinhardt. Which attention heads matter for in-context learning?, 2025. URL https://arxiv.org/abs/2502.14010.

Kang Min Yoo, Junyeob Kim, Hyuhng Joon Kim, Hyunsoo Cho, Hwiyeol Jo, Sang-Woo Lee, Sang-goo Lee, and Taeuk Kim. Ground-truth labels matter: A deeper look into input-label demonstrations. In Yoav Goldberg, Zornitsa Kozareva, and Yue Zhang (eds.), *Proceedings of the 2022 Conference on Empirical Methods in Natural Language Processing*, pp. 2422–2437, Abu Dhabi, United Arab Emirates, December 2022. Association for Computational Linguistics. doi: 10.18653/v1/2022.emnlp-main.155. URL https://aclanthology.org/2022.emnlp-main.155/.

Wenting Zhao, Xiang Ren, Jack Hessel, Claire Cardie, Yejin Choi, and Yuntian Deng. Wildchat: 1m chatGPT interaction logs in the wild. In *The Twelfth International Conference on Learning Representations*, 2024. URL https://openreview.net/forum?id=Bl8u7ZRlbM.

Ziqian Zhong, Ziming Liu, Max Tegmark, and Jacob Andreas. The clock and the pizza: Two stories in mechanistic explanation of neural networks. In *Thirty-seventh Conference on Neural Information Processing Systems*, 2023. URL https://openreview.net/forum?id=S5wmbQc1We.

Tianyi Zhou, Deqing Fu, Vatsal Sharan, and Robin Jia. Pre-trained large language models use fourier features to compute addition. In *The Thirty-eighth Annual Conference on Neural Information Processing Systems*, 2024. URL https://openreview.net/forum?id=i4MutM2TZb.

A Limitations

Regarding circuit discovery experiments (§3, §D and §E), the identified circuit is limited as it does not perfectly satisfy the faithfulness and completeness criteria, even with our best efforts. This challenge arises because achieving simultaneous satisfaction of faithfulness, completeness, and minimality is difficult, as these criteria often regulate each other. Moreover, number tokens are often mapped into a sinusoidal (Fourier) feature space rather than a linear space in language models (Nanda et al., 2023; Zhong et al., 2023; Zhou et al., 2024), which further complicates our interpretability analysis.

Regarding circuit analysis (§4 and §F), we mainly used causal intervention methods and examine the causal effect of attention heads on naive prompts. Future work could provide deeper mechanistic insights by analyzing the query-key and output-value circuits within these heads (Elhage et al., 2021), or by investigating the role of MLP layers in the overall mechanism.

Regarding task generalization experiments (§5 and §G), our current scope is limited to two-step tasks where the second step involves a shifting-related function. We anticipate that the function induction mechanism could operate on a broader spectrum of functions, which could be investigated in future work. Additionally, the task pairs we investigated are synthetic or algorithmic; further exploration of the role of function induction heads on naturally occurring texts would be highly valuable.

B Induction Head Mechanism and Function Induction Mechanism

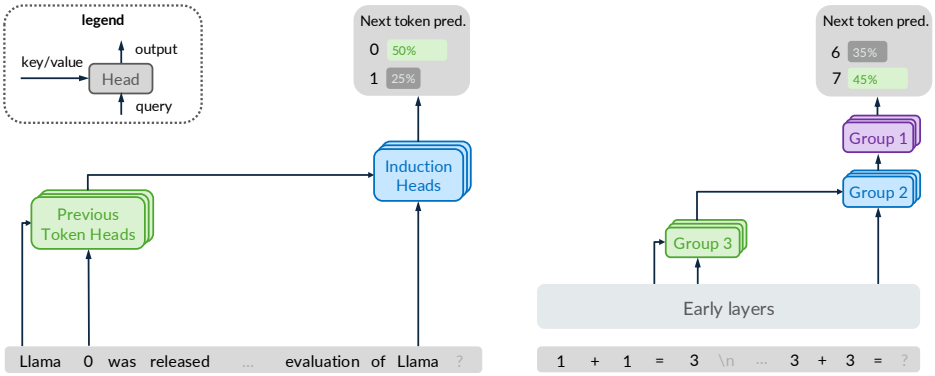

Figure 8: **Comparing Induction Head (Left) and Function Induction (Right).**

Comparing Induction Head and Function Induction. Fig. 8 provides a side-by-side visualization of the induction head mechanism (Olsson et al., 2022) and the hypothesized function induction mechanism (§3.2), demonstrating their structural similarity and explaining the basis for our hypothesis.

To provide a more concrete example on how induction heads work, consider the hypothetical scenario where a language model is completing the prompt: "Llama 0 was released in 2022. This paper presents an extensive evaluation of Llama ..." When the model first encounters an uncommon phrase, *e.g.*, "Llama 0", a previous token head will attend to "Llama" and register the information that "Llama appears before 0" at the position of "0". Later on, when "Llama" appears in the context again, an induction head will retrieve this piece of information from position of "0" and increase the likelihood of generating "0" as the next token. This induction head mechanism informs our hypothesis on function induction in §3.2 and the collaborative interaction between previous token heads and function induction heads in Fig. 8 (Right).

Relevance to In-context Learning with False Demonstrations. Various prior works investigate how language models handle false, random, or perturbed demonstrations in in-context learning (Min et al., 2022b; Yoo et al., 2022; Wei et al., 2024; Lyu et al., 2023; Lin & Lee, 2024). Notably, Halawi et al. (2023) adopted an interpretability approach, observing the *overthinking* behavior of models (*i.e.*, models draft truthful answers at early layers and flip them to untruthful answers at late layers), and identified *false induction heads* that are responsible for copying the untruthful answers from the ICL examples.

Our analysis of off-by-one addition was largely motivated by these studies. Here we revisit the findings of Halawi et al. (2023) along with ours, using a unified view of two-step tasks, *i.e.*, $z = f(g(x))$. In Halawi et al. (2023), the first step, $y = g(x)$ is typically a text classification task, *e.g.*, news topic classification, and the second step, $z = f(y)$ is a permutation of the labels, *e.g.*, {Business→Sci/Tech, Sci/Tech→World, World→Sport, Sports→Business}. In our work, $y = g(x)$ is standard addition, and $z = f(y)$ is a +1 function.

In this view, our findings with off-by-one addition are consistent with those in Halawi et al. (2023), while also advancing the understanding in several aspects: (1) In both cases, language models decompose the task into two steps, and induce the second step based on the results of the first step. The second step could be either a conditional copy-paste function, *e.g.*, a permutation of labels, *or* an algorithmic function, *e.g.*, a +1 function. The latter represents a novel finding of this study, demonstrating that the second step can exhibit forms more complex than copy-paste operations. (2) Our path patching procedure has led us to identify two additional group of heads (consolidation heads and previous token heads) that are involved in handling false demonstrations. (3) Our work also suggests that the strategy to improve truthfulness by zeroing out false induction heads or function induction heads may have unintended consequences on models' positive capabilities, given their positive contributions to the cipher task and the base-8 addition task.

Related to the view of two-step tasks, Jain et al. (2024) demonstrate that models learn a "wrapper" function g over an existing function f in a sequential fine-tuning setting. Our work and Halawi et al. (2023) suggest that language models demonstrate simple forms of this behavior with in-context learning as well.

C Off-by-One Addition Evaluation

Models. In §2 we evaluated six recent language models on the task of off-by-one addition. In Table 4 we provide details of these models.

Model Name	Huggingface Identifier	Reference	Tokenization 0-9	Tokenization 0-999
Llama-2 (7B)	meta-llama/Llama-2-7b-hf	Touvron et al. (2023)	✓	
Mistral-v0.1 (7B)	mistralai/Mistral-7B-v0.1	Jiang et al. (2023)	✓	
Gemma-2 (9B)	google/gemma-2-9b	Gemma Team (2024)	✓	
Qwen-2.5 (7B)	Qwen/Qwen2.5-7B	Yang et al. (2024a)	✓	
Llama-3 (8B)	meta-llama/Meta-Llama-3-8B	Grattafiori et al. (2024)		✓
Phi-4 (14B)	microsoft/phi-4	Abdin et al. (2024)		✓

Table 4: **Models Evaluated on Off-by-One Addition.** "0-9" means the model uses digit-level tokenization for numbers, *e.g.*, "123" is tokenized into ["1","2","3"], "0-999" means all numbers smaller than 1000 are considered one single token, *e.g.*, "123" is tokenized into ["123"].

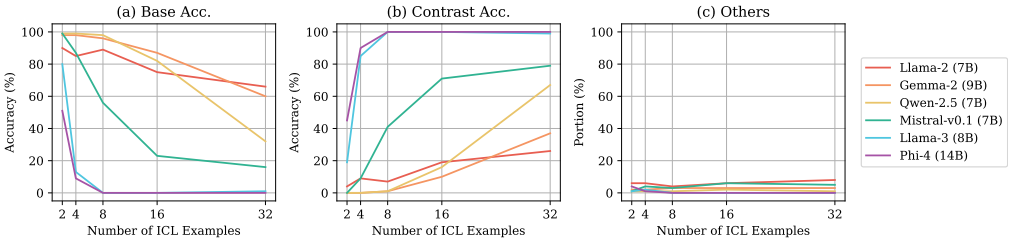

Figure 9: **Off-by-One Addition Evaluation, Reporting Base Accuracy.**

Reporting base and contrast accuracy. Previously in Fig. 1, we reported the accuracy of off-by-one addition (*i.e.*, the percentage of time that the model outputs 7 when given 3+3). In Fig. 9(a) we additionally report the accuracy of standard addition (*e.g.*, "3+3=6"), when the models are given the contrast prompt (*e.g.*, "1+1=3\n2+2=5"). We find that the base accuracy consistently decrease with

more in-context learning examples. In Fig. 9(c), we show that models may also output numbers that are incorrect either in standard addition or off-by-one addition (*i.e.*, neither "6" or "7").

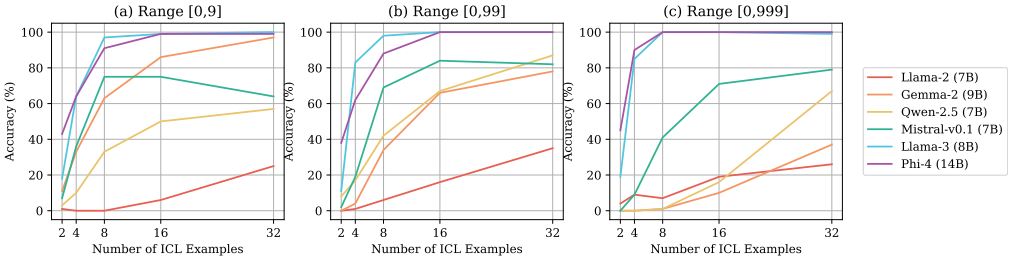

Figure 10: **Off-by-One Addition Evaluation, Using Smaller Number Ranges.**

Results in a smaller number range. Previously in Fig. 1, we reported results when the operands were sampled from the range of [0,999]. In Fig. 10, we additionally report results when sampling from the range of [0,9] and [0,99]. For two models using 0-9 tokenization (`Gemma-2 (9B)` and `Qwen-2.5 (7B)`), the performance drops with larger number ranges. For the remaining models, the performance remains stable regardless of the number ranges.[4]

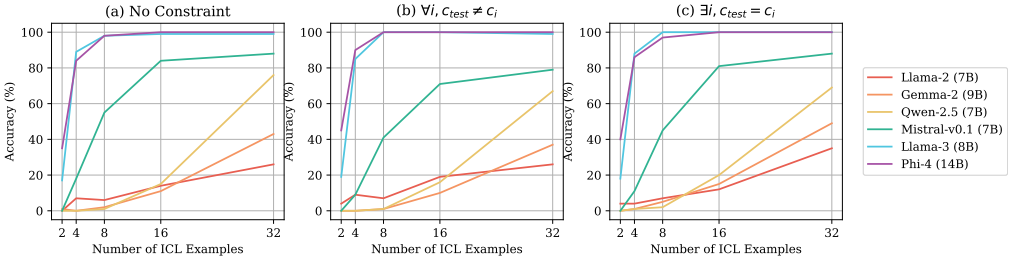

Figure 11: **Off-by-One Addition Evaluation, Different Sampling Constraints.**

Results with/without the constraint of $c_{test} \neq c_i$. Previously in §2 we deliberately impose the constraint that $\forall i, c_{test} \neq c_i$. This is to rule out the possibility that language models perform off-by-one addition via copying c_{test} from previous contexts. In Fig. 11, we compare the results of two additional sampling strategies: (1) no constraint on c_{test} and c_i; (2) $\exists i, c_{test} = c_i$. By comparing Fig. 11(b) and (c) we see that for `Mistral-v0.1 (7B)` and `Gemma-2 (9B)`, the accuracy is higher when $\exists i, c_{test} = c_i$. This observation implies that these two models leverages copy-paste induction more than function induction in performing off-by-one addition, though more rigorous analysis is required to draw a conclusion.

Results with off-by-k addition. In Fig. 12-13, we present 32-shot off-by-k addition results with various offsets k using `Gemma-2 (9B)` and `Llama-3 (8B)` respectively.[5] One consistent trend is that models struggle more with offsets k of larger absolute values. While `Llama-3 (8B)` generally outperforms `Gemma-2 (9B)`, `Gemma-2 (9B)` demonstrates strong performance when $k = \pm 10$, potentially due to its adoption of 0-9 tokenization. An additional observation reveals that `Gemma-2 (9B)` typically achieves stronger performance with even values of k compared to odd values.

[4]We chose `Gemma-2 (9B)` as the default model in our study because (1) we focused on the range of [0,9] in early stage of this work to prioritize simplicity, and `Gemma-2 (9B)` performs competitively in this setting; (2) `Qwen-2.5 (7B)`, `Llama-3 (8B)`, `Phi-4 (14B)` were not released or integrated into `transformer-lens` at that time. We acknowledge this experimental design limitation and address it by interpreting `Llama-3 (8B)` and `Mistral-v0.1 (7B)` in §D.

[5]The visualization of Fig. 12-13 was inspired by Prabhakar et al. (2024).

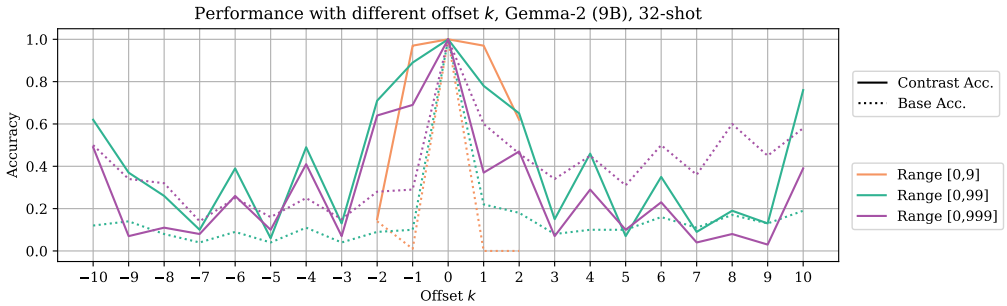

Figure 12: **Off-by-k Addition Evaluation, `Gemma-2 (9B)`**

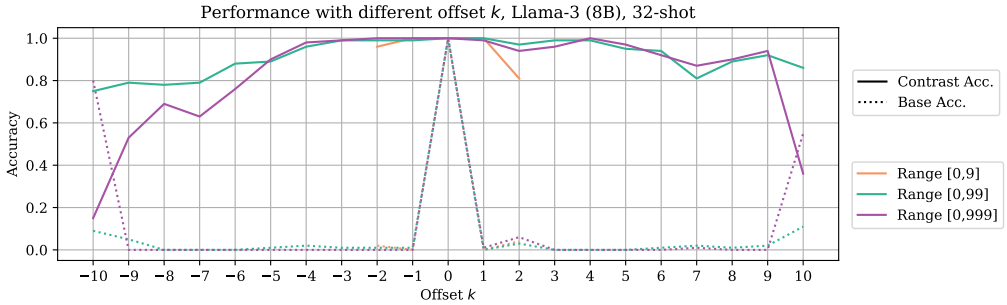

Figure 13: **Off-by-k Addition Evaluation, `Llama-3 (8B)`**

D Circuit Discovery

D.1 Relative Logit Diff

§3.1 introduced r, the relative logit difference, to measure the effect of a replacement during circuit discovery. We now elaborate on this formula to enhance clarity.

$$r = \frac{F(M', x_{cont}) - F(M, x_{cont})}{F(M, x_{cont}) - F(M, x_{base})} \tag{1}$$

$$= \frac{[M'(y_{base}|x_{cont}) - M'(y_{cont}|x_{cont})] - [M(y_{base}|x_{cont}) - M(y_{cont}|x_{cont})]}{[M(y_{base}|x_{cont}) - M(y_{cont}|x_{cont})] - [M(y_{base}|x_{base}) - M(y_{cont}|x_{base})]} \tag{2}$$

D.2 Identified Heads

In the main paper, we focus on interpreting `Gemma-2 (9B)`. To explore the universality of the mechanism, we additionally conduct path patching with `Llama-3 (8B)`, `Llama-2 (7B)` and `Mistral-v0.1 (7B)`. We list the identified attention heads below.

D.2.1 `Gemma-2 (9B)`

`Gemma-2 (9B)` has 42 layers and 16 heads per layer. Path patching experiments were conducted with 4-shot off-by-one addition with numbers sampled from range [0,9].

- Consolidation Heads: H41.4, H41.5, H40.11, H40.12;
- Function Induction (FI) Heads: H39.7, H39.12, H36.7, H32.1, H32.6, H25.13;
- Previous Token (PT) Heads: H38.6, H38.7, H38.9, H35.14, H35.9, H31.4, H31.5, H29.5.

D.2.2 `Llama-3 (8B)`

`Llama-3 (8B)` has 32 layers and 32 heads per layer. Path patching experiments were conducted with 4-shot off-by-one addition with numbers sampled from range [0,999]. We visualize the path patching results in Fig. 14.

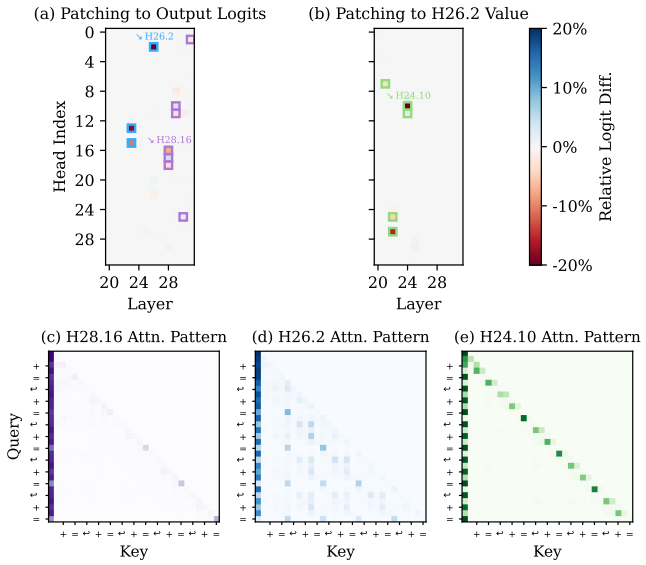

Figure 14: **Circuit Discovery with `Llama-3 (8B)`.** Results are consistent with those with `Gemma-2 (9B)` in Fig. 2.

- Consolidation Heads: H31.1, H30.25, H29.11, H29.10, H28.16, H28.17, H28.18;
- Function Induction (FI) Heads: H26.2, H23.13, H23.15;
- Previous Token (PT) Heads: H24.10, H24.11, H22.25, H22.27, H21.7.

D.2.3 `Mistral-v0.1 (7B)`

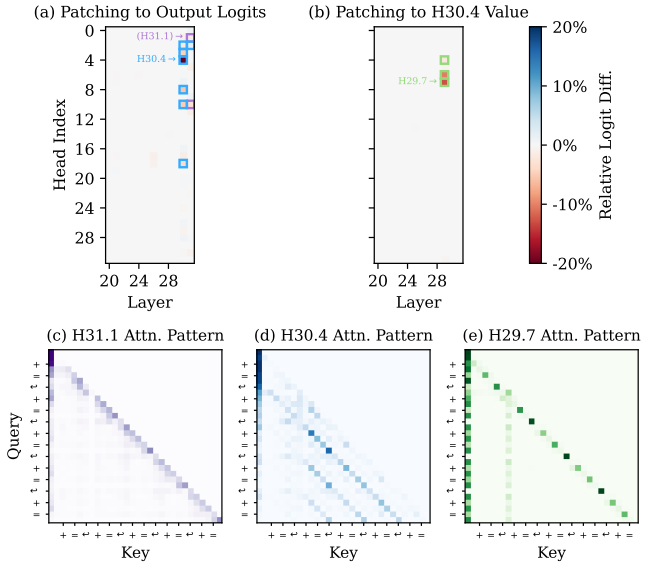

Figure 15: **Circuit Discovery with `Mistral-v0.1 (7B)`.** Results are mostly consistent with those with `Gemma-2 (9B)` in Fig. 2, with the exception of the consolidation heads showing weaker signals.

`Mistral-v0.1 (7B)` has 32 layers and 32 heads per layer. Path patching experiments were conducted with 4-shot off-by-one addition with numbers sampled from range [0,9]. We visualize the results in Fig. 15. For the two consolidation heads in the list below, they show weaker effect and attend to both the current token and some other tokens, which slightly deviates from our findings with `Gemma-2 (9B)`. Apart from this, the results using `Mistral-v0.1` are consistent with other models.

- Consolidation Heads: (H31.10), (H31.1)
- Function Induction (FI) Heads: H30.2, H30.3, H30.4, H30.8, H30.10, H30.18, H31.2
- Previous Token (PT) Heads: H29.4, H29.6, H29.7.

D.2.4 `Llama-2 (7B)`

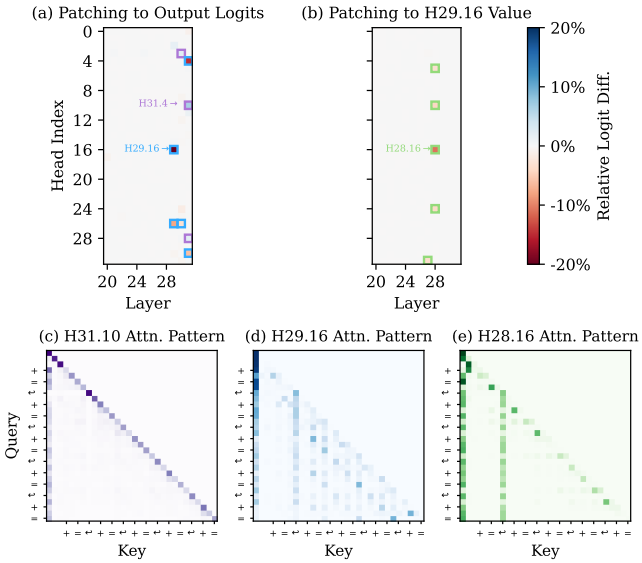

Figure 16: **Circuit Discovery with `Llama-2 (7B)`.** Results are mostly consistent with those with `Gemma-2 (9B)` in Fig. 2.

`Llama-2 (7B)` has 32 layers and 32 heads per layer. Path patching experiments were conducted with 4-shot off-by-one addition with numbers sampled from range [0,9]. We visualize the results in Fig. 16.

All three groups of heads are present in `Llama-2 (7B)`. However, we notice two small variations compared to the circuit in `Gemma-2 (9B)`. **(1)** We identified H16.24 that achieves $r = 2.12\%$, but its attention pattern doesn't fit that of a consolidation head or a function induction head. Since 2.12% is slightly above the 2% threshold we set, we consider this noise; **(2)** One previous token head (H29.1) no longer attends to the "=" immediately before the answer token c_i at the token c_i. Instead, it attends to the "=" token one ICL example away.

To discuss our findings with those of Todd et al. (2024) with a common ground, we extract the list of FV heads by selecting the 10 heads with the highest absolute average indirect effect (AIE) from Fig. 19 in Todd et al. (2024). These heads are concentrated in early-middle layers (before layer 20), whereas our FI heads appear in late layers (layers 29-31). There is no overlap between the two sets.

- Consolidation Heads: H31.28, H31.10, H30.3;
- Function Induction (FI) Heads: H31.30, H31.4, H29.26, H29.16, H30.26, H30.3;
- Previous Token (PT) Heads: H30.13, H29.1, H28.5, H28.10, H28.16, H28.24, H27.31;
- Miscellaneous Heads: H16.24;
- Function Vector Heads (Todd et al., 2024): H9.25, H11.2, H11.18, H12.15, H12.18, H12.28, H13.7, H14.1, H14.16, H16.10.

D.3 Additional Interpretability Analysis

D.3.1 Logit Lens Analysis

In this section, we apply logit lens (nostalgebraist, 2020), a widely-adopted interpretability method, to off-by-one addition. This involves directly computing the logits from intermediate layer representations using the final layer norm and the final unembedding layer.

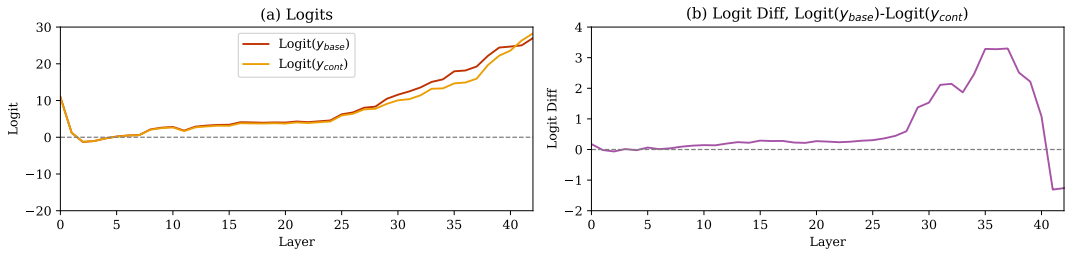

Figure 17: **Logit Lens Results when Using x_{cont} as the Input Prompt.**

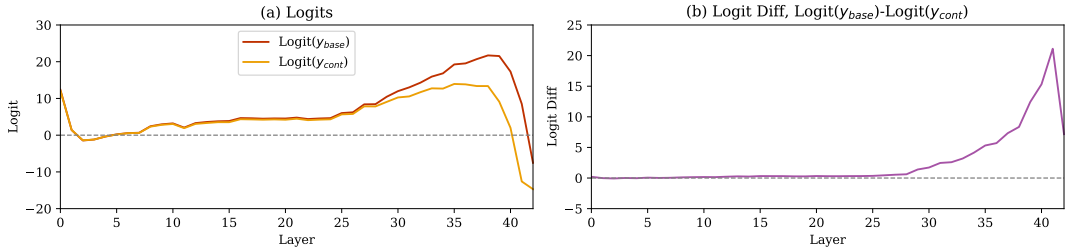

Figure 18: **Logit Lens Results when Using x_{base} as the Input Prompt.**

We use `Gemma-2 (9B)` and 100 16-shot examples in this set of experiments. In Fig. 17, we report the logits of the base answer y_{base} (*i.e.*, model outputting 3+3=**6**), the contrast answer y_{cont} (*i.e.*, model outputting 3+3=**7**) and their differences, computed using the contrast prompt x_{cont} (*i.e.*, 1+1=3) as model input. In Fig. 18, we repeat the experiments using x_{base} (*i.e.*, 1+1=2) as the input prompt.

By comparing Fig. 17(a) and Fig. 18(a), we find that the curves in the two subplots begin to diverge notably after layer 25. This supports our claim that the model performs standard addition in the early layers and apply the +1 function in late layers.

Additionally, by comparing Fig. 17(b) and Fig. 18(b), we find that the logit diff decreases sharply after layer 38 in Fig. 17(b), a phenomenon absent in Fig. 18(b). This is consistent with our findings that H39.7 and H39.12 contribute significantly to writing out the +1 function to the residual stream.

D.3.2 Activation Patching Analysis

In this section, we apply activation patching (Meng et al., 2022) to off-by-one addition. We performed this analysis in the early stages of our work to gather initial intuitions and signals for our problem, before transitioning to path patching for a more fine-grained understanding of the model's internal computation.

We use `Gemma-2 (9B)` and 100 4-shot examples in this set of experiments. First, we run forward passes for both the base prompt x_{base} and the contrast prompt x_{cont}. We store the activations and then replace the activations in the x_{cont} forward pass with corresponding activations in the x_{base} forward pass. We consider activation patching by token (Fig. 19) and by head (Fig. 20). We report the ratio $r' = 1 + r = \frac{F(M', x_{cont}) - F(M, x_{base})}{F(M, x_{cont}) - F(M, x_{base})}$ in these figures following previous works. We scaled the colormap in the figures to the range of [-50%, 50%] for clear visualization.

Fig. 19(a) visualizes the information flow from in-context examples to the residual stream of the last " =" token. Additionally, Figure 19(b) highlights several layers, specifically layers 32, 36, and 39 at the last "=" token, and layers 35 and 38 at the answer tokens c_i in the in-context examples. This aligns with the FI heads (H36.7, H39.7, H39.12) and PT heads (H35.9, H35.14, H38.6, H38.7, H38.9) identified in §3.2. Figure 19(c) further reveals that MLP layers also play critical roles at certain positions. It is possible that FI heads write the +1 function to the residual stream, with subsequent attention and MLP layers involved in the execution of the +1 function. This hypothesis is inspired by prior observations of how MLP layers in transformer models are involved in arithmetic operations (Nanda et al., 2023; Stolfo et al., 2023). In this work, we limit our focus to attention heads, deferring further analysis of MLP layers to future work.

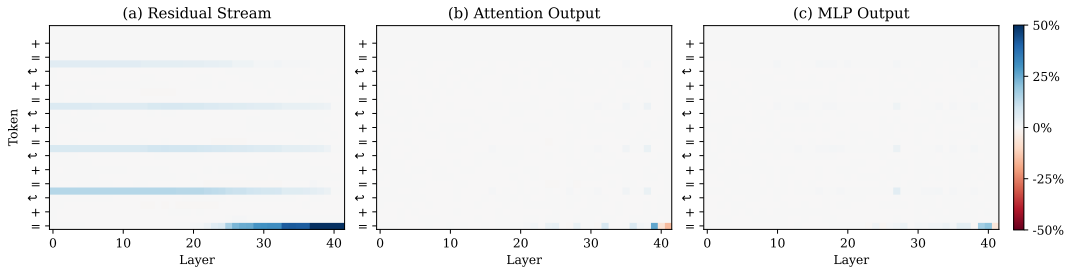

Figure 19: **Activation Patching By Token.**

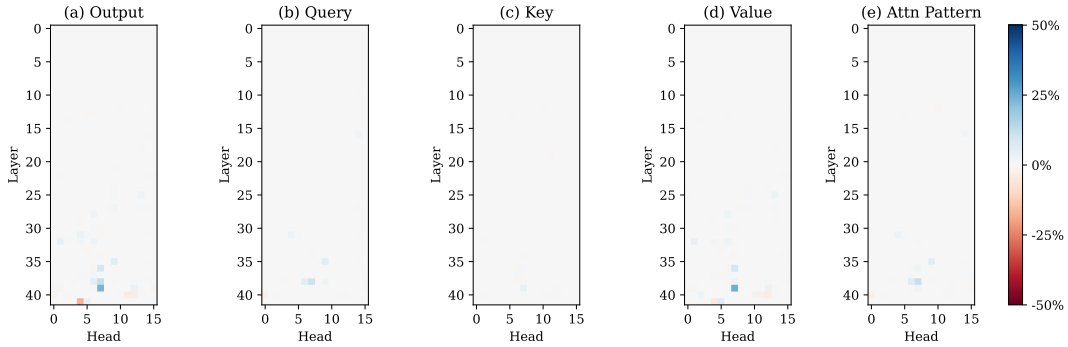

Figure 20: **Activation Patching By Head.**

Results in Fig. 20 guide and complement our path patching experiments in §3.2. The identified PT heads (H35.9, H38.6, H38.7, H38.9) are highlighted in Fig. 20(b) and the FI heads (H36.7, H39.7, H39.12, H32.1, H25.13) are highlighted in Fig. 20(d).

D.3.3 Alternative Head Ablation Methods

In the main paper, we "ablate" or "knock out" a head by replacing its output in the x_{cont} forward pass with the corresponding head output in the x_{base} forward pass. This instance-specific ablation approach is adopted to better isolate the +1 function computation in each instance. However, this differs from ablation methods commonly used in interpretability work, such as zero ablation (Halawi et al., 2023) or mean ablation (Wang et al., 2023).

To demonstrate the consistency of our findings across different ablation settings, we repeated the experiment in Fig. 4 using zero ablation and mean ablation. For mean ablation, we averaged head outputs at the final "=" token from 100 standard addition examples. We found that in all ablation settings (zero ablation, mean ablation, and our instance-specific ablation), the contrast accuracy reduced to 0% and the base accuracy increased to 100% after ablation.

E Circuit Evaluation

In §4, we primarily validated the identified circuit using head ablation experiments and causal effect visualizations. Wang et al. (2023) proposed a more rigorous framework for circuit evaluation, based on **faithfulness**, **completeness**, and **minimality**. In the following, we evaluate the identified circuit according to these metrics. Note that we focus on interpreting the "off-by-one" component of the task, rather than the standard addition component. Hence, these circuit evaluation metrics are adapted accordingly to use $F(M, x_{base})$ as a reference point.

The **faithfulness** metric measures whether a circuit C has a similar performance to the full model M, *i.e.*, whether $F(C, x_{cont})$ is close to $F(M, x_{cont})$, with $F(C, x)$ defined earlier in §3.1. We find that $F(M, x_{base}) = 7.17$, $F(M, x_{cont}) = -1.26$, and $F(C, x_{cont}) = 0.56$, suggesting that C recovers $\frac{7.17-0.56}{7.17-(-1.26)} = 78.4\%$ of the performance of M.

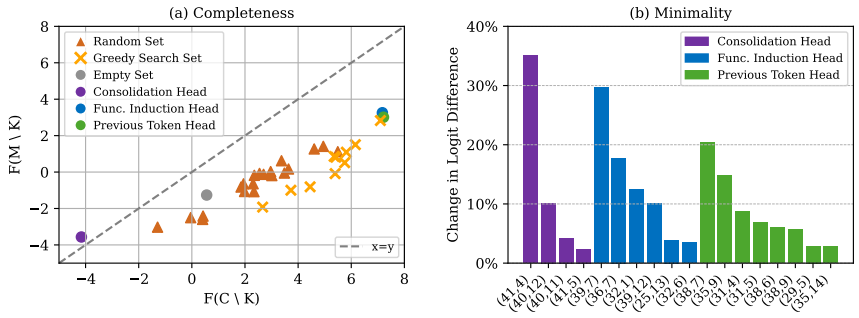

Figure 21: **Circuit Evaluation.**

The **completeness** criterion evaluates whether for each subset $K \subseteq C$, the difference between $F(C \backslash K, x_{cont})$ and $F(M \backslash K, x_{cont})$ is small. In the following, we will omit the x_{cont} term for brevity. We use various different sets (*e.g.*, randomly or greedily selected) as K and report the results in Fig. 4(b). We find most points representing $(F(C \backslash K), F(M \backslash K))$ fall slightly below the $x = y$ line, while maintaining a monotonic trend, suggesting that the circuit C is partially complete. This represents the best we can achieve with our current methodology. We also find that when K is the set of all PT heads or all FI heads, both $f(C \backslash K)$ and $f(M \backslash K)$ are high, suggesting that the model favors y_{base} in next-token generation (*i.e.*, 3+3=6) and switches back to standard addition under these ablation conditions. These observations are consistent with our function induction hypothesis.

Lastly, the **minimality** criterion measures whether each head v in C is necessary, by seeking a subset $K \subseteq C \backslash \{v\}$ that has a high score of $|F(C \backslash (K \cup \{v\})) - F(C \backslash K)|$. We manually constructed the K sets for this purpose. As shown in Fig. 4(c), each head in C is relevant to the task and has a non-trivial effect (>2%) in performing off-by-one addition.

E.1 Improving the Identified Circuit with Local Search

Our circuit evaluation above is based on the circuit discovery procedure described in §3.2, where we used a 2% threshold to highlight relevant heads and ensure that the number of heads involved is manageable. This evaluation reveals that circuit C achieves a faithfulness score of 78.4%, recovering a substantial portion of the model's behavior but suggesting we may have missed several heads responsible for the remaining 22%.

To address this, we employ a local search method. Specifically, we enumerate heads not in C (*i.e.*, $v \in M \backslash C$), add each to C to form a new circuit $C' = C \cup \{v\}$, and evaluate the faithfulness score of C'. We identify 7 heads that produce faithfulness score changes greater than 1.5%, which we report in Table 5. These include 6 heads (H37.6, H38.8, H40.0, H37.4, H24.9, H32.4) that increase the faithfulness score and 1 head (H36.6) that decreases it.

Including the 6 score-increasing heads in C (denoted C_6) raises the faithfulness score to 89%. Including all 7 heads By including the 7 heads (denoted C_7) reduces the faithfulness score to 82%, which still exceeds the 78% achieved by the original circuit C.

We further examine the attention pattern of these heads. H37.6, H24.9, H32.4, and H36.6 exhibit patterns consistent with FI heads, while H38.8 fits the description of consolidation heads. However, H40.0 and H37.4 do not fit any head group in our function induction hypothesis. At "=" tokens, H40.0 attends to itself in the forward pass of x_{base} but not in the forward pass of x_{cont}, likely suppressing the standard addition answer (y_{base}) by weakening its consolidation. H37.4 attends to "=" tokens in previous ICL examples at each "=", likely retrieving the consolidation signal from earlier ICL examples.

	Δ Faithfulness (%)	Rel. Logit Diff r (%)
H37.6	3.13	0.88
H38.8	2.33	0.55
H40.0	2.29	-1.26
H37.4	1.96	0.39
H24.9	1.86	1.64
H32.4	1.67	1.29
H36.6	-3.44	-1.15

Table 5: **Identifying Missing Heads with Local Search.** The "Rel. Logit Diff r" columns reports the relative effect r of these heads when patching to the final logits (§3.2). Previously we set a threshold of 2% and hence these heads were not identified.

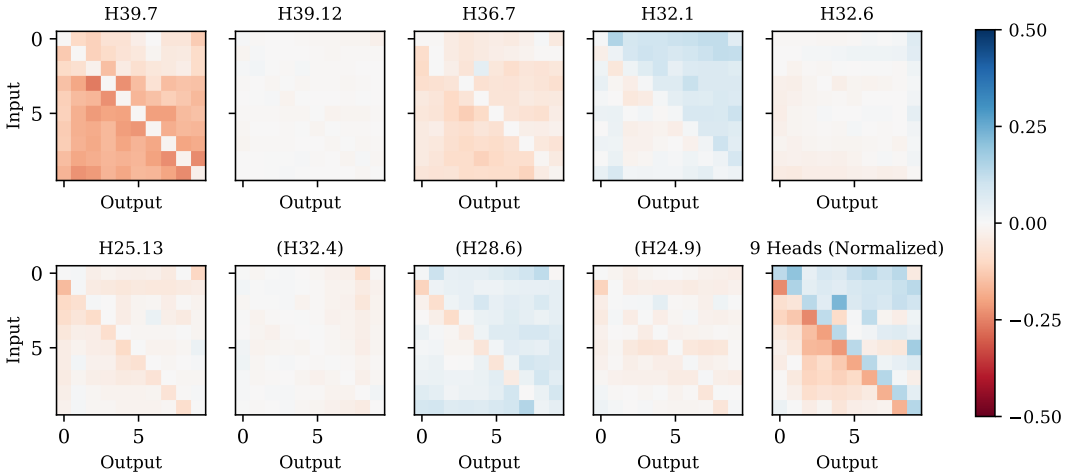

Figure 22: **Individual and Overall Effect of Identified FI Heads (Standard Addition).**

F Circuit Analysis

Due to space limit, we mainly perform circuit analysis on function induction (FI) heads and present the most notable findings in the main paper (§4). In this section, we discuss remaining findings on FI heads in §F.1. We also present additional analysis on consolidation heads in §F.2 and previous token (PT) heads in §F.3.

F.1 Function Induction (FI) Heads

What do FI heads write out in standard addition? Our function vector style analysis in §4 primarily focuses on what FI heads write out in off-by-one addition. However, these heads may also assume roles in standard addition. To investigate this, we add the FI head outputs in the $M(.|x_{base})$ to the naive prompt x_{naive}, and visualize the effect in Fig. 22. By comparing Fig. 5 and Fig. 22, we observe that most FI heads contribute meaningful but distinct information in standard addition, with H39.12 being an exception given its minimal effect in standard addition. The aggregated effect in the bottom-right panel in Fig. 22 suggests that FI heads collectively suppress $x - 1$ and promote x in standard addition.

One possibility is that FI heads reinforce the answer x, or double-check it by performing $(x - 1) + 1$ in standard addition. In contrast, during off-by-one addition, the standard addition answers are first "locked in" after early layers, and the FI heads are repurposed to perform +1. We leave further investigation of this phenomenon to future work.

What do FI heads write out in off-by-k addition? Previously in Fig. 7, we demonstrated how the effect of H39.7 and H25.13 changes with respect to different offset k. In Fig. 23-25 we report the

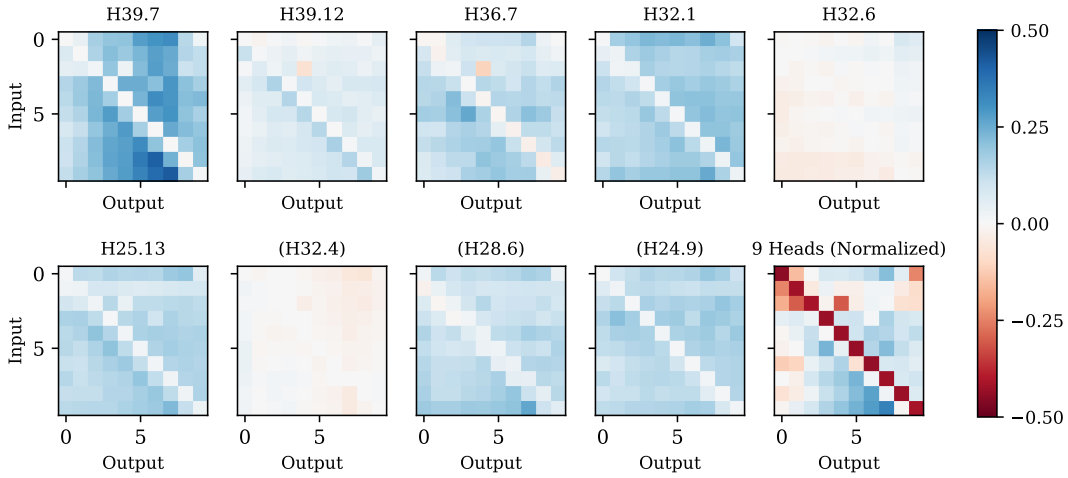

Figure 23: **Individual and Overall Effect of FI Heads in Off-by-k Addition, $k = -2$.**

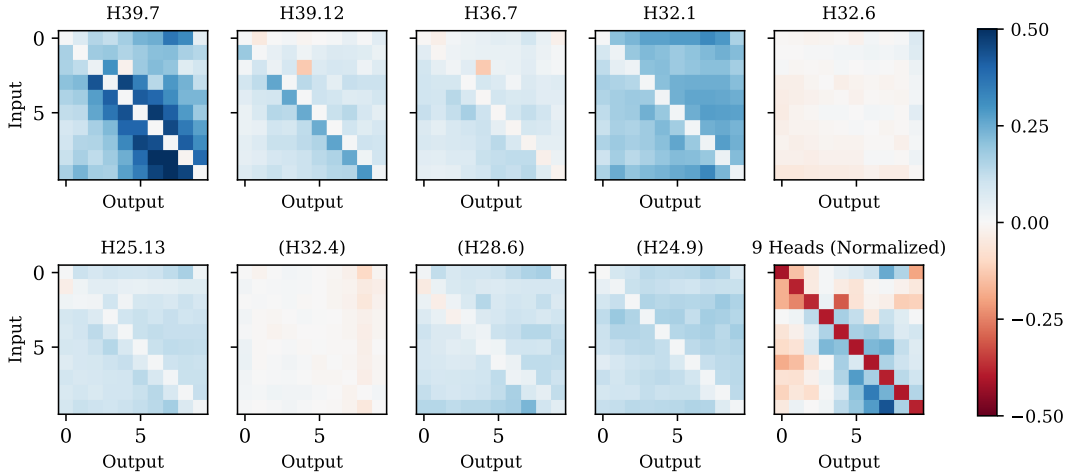

Figure 24: **Individual and Overall Effect of FI Heads in Off-by-k Addition, $k = -1$.**

effect of all nine heads when $k = -2, -1, 2$. We find that for some heads (*e.g.*, H32.1 and H24.9), their effect of suppressing x remains consistent across different k values. For other heads (*e.g.*, H39.7, H39.12, H25.13), their effect changes accordingly with k.

F.2 Consolidation Heads

We repeat our function vector style analysis from §4, but this time use the consolidation heads as the subject. Concretely, we patch the outputs of these heads from the last token residual stream in off-by-one addition (*e.g.*, "1+1=3\n2+2=5\n3+3=?") to the naive prompts (*e.g.*, "2=2\n3=?"). We report the effect of this intervention on the output logits in Fig. 26.

We observe that three of these heads (H41.4, H40.11, H40.12) are suppressing answers other than x, and one head (H41.5) is promoting answers other than x. Their aggregated effect leads to promoting x and suppressing $x + 1$, which counters the effect brought by FI heads discussed in Fig. 5.

Discussion. We name these heads as "consolidation heads" based on three observations: **(1)** they appear in the final two layers; **(2)** they attend exclusively to the current token and the <bos> token, suggesting that they mainly process information locally at the current token; **(3)** our causal analysis in Fig. 26 shows that some of them are promoting 3+3=6 and some are promoting 3+3=7 in off-by-one addition, suggesting that they are weighing the two possible outputs collaboratively.

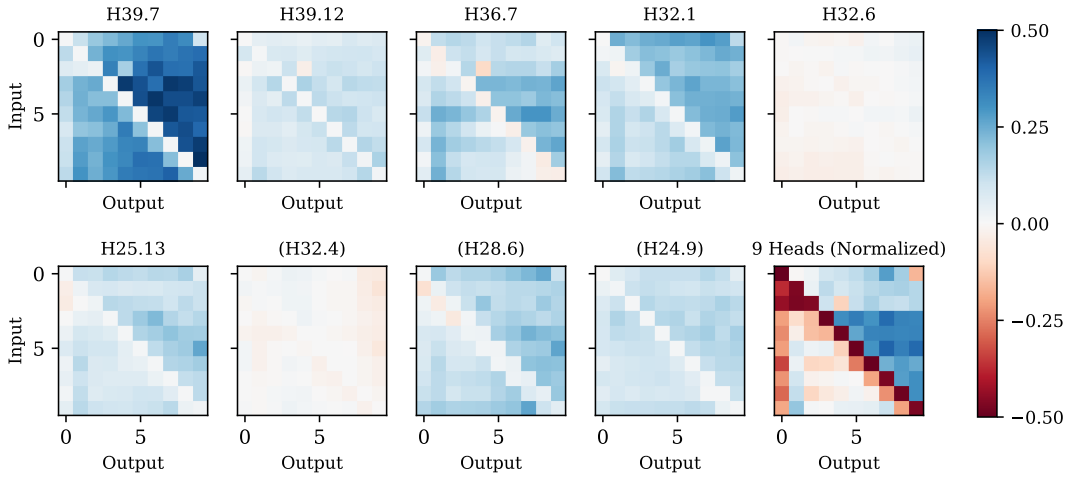

Figure 25: **Individual and Overall Effect of FI Heads in Off-by-k Addition, $k = 2$.**

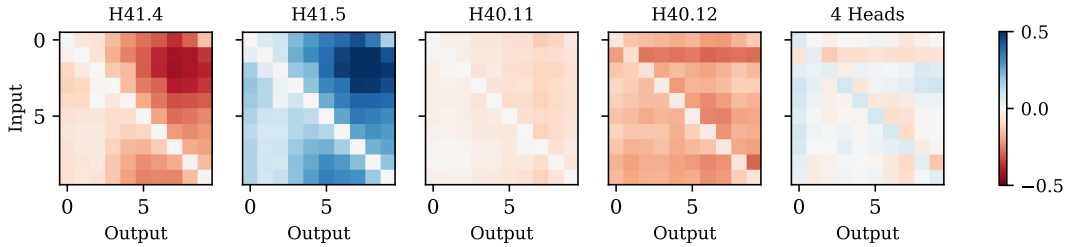

Figure 26: **Causal Effect of Consolidation Heads.** The aggregated effect of consolidation heads counter the effect of FI heads by promoting x and suppressing $x + 1$.

Despite these observations, our understanding on the exact role of these heads, and why they emerge, remain limited. We believe it relates to the broader phenomenon of "negative" behavior in language models, which has been noted as a challenge for current interpretability methods (Sharkey et al., 2025). We hope future work will present a finer-grained interpretation of these heads.

F.3 Previous Token (PT) Heads

	Off-by-one Addition		Off-by-two Addition	
Prompt Setting	Base Acc	Cont. Acc	Base Acc	Cont. Acc
Base Prompt	1.00	0.00	1.00	0.00
Contrast Prompt	0.11	0.86	0.04	0.46
Contrast Prompt (Ablate PT Heads)	0.96	0.04	0.95	0.01
Contrast Prompt (Ablate 8 Random Heads)	0.09	0.89	0.05	0.46

Table 6: **Head Ablation Experiments with Previous Token Heads.**

Head Ablation Experiments. To validate the role of previous token heads, we first repeat the head ablation experiments in Fig. 4, but we ablated previous token heads instead. We consider both off-by-one addition and off-by-two addition, and use 16-shots in the prompt. We report the results in Table 6. Ablating the previous tokens heads almost completely restores the model's default behavior. This supports our hypothesis that these heads are critical for inducing the +1 function.

Causal Effect. To further investigate the causal effect of previous token (PT) heads, we adapt our causal analysis method previously used for FI heads and consolidation heads. For example, consider the off-by-one addition prompt, "1+1=3\n2+2=5\n3+3=?", we extract the PT head outputs at the tokens marked in brown, average the outputs over the two tokens (3 and 5), and add them to the

forward pass of the naive prompt "2=2\n3=?", at the token 2 marked in brown. In our experiments, we scaled this explanatory example to 100 4-shot examples of off-by-one addition to extract the PT head outputs.

We report the causal effect of these PT head outputs in Fig. 27. Similar to the findings with FI heads, we find that each PT head conveys distinct information. For example, H38.7 promotes $x \pm 1$ and $x \pm 2$, H35.14 promotes $x+1$ and suppresses $x-1$. Collectively, these heads suppress x and promote $x+1$, which aligns with the hypothesized role of PT heads. Unexpectedly, these heads also promotes $x-1$. We attribute this to the task shift from off-by-one addition and the naive prompt, and the token-level averaging operation we employ which may cause loss of information.

Pairs of Heads with Countering Effect. We notice that two pairs of PT head (H38.6/7 and H31.4/5) demonstrate opposing patterns, and they happen to be in the same group in group query attention. Similarly, two consolidation heads (H41.4/5; Fig. 26) have a similar countering effect. Hence we hypothesize that group query attention may help these heads develop countering or hedging behaviors.

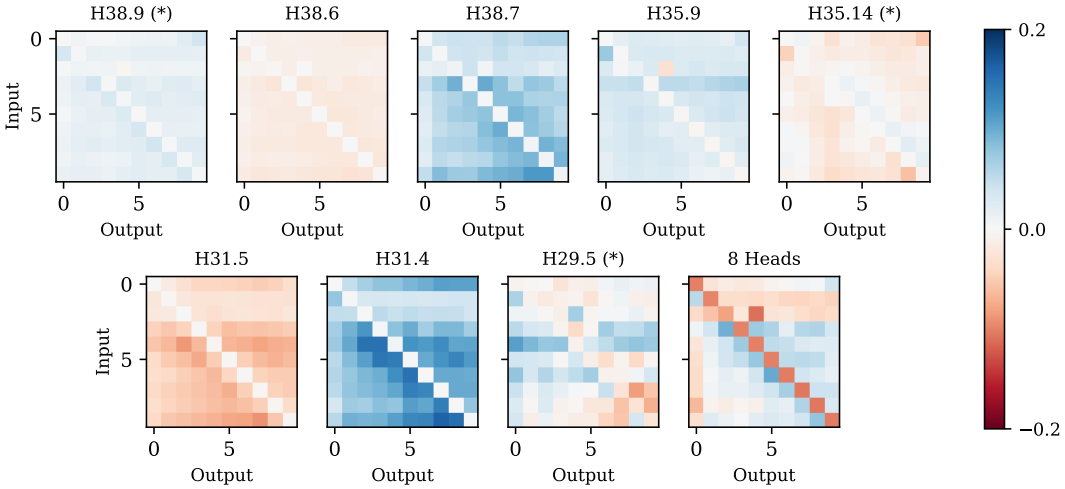

Figure 27: **Causal Effect of Previous Token Heads.** (*) Effects of H38.9, H35.14 and H29.5 are rescaled to [-0.02, 0.02] to make the patterns more readable.

G Task Generalization

G.1 Tasks and Data Preparation

In this section we describe the task pairs we used in §5 with more details.

Off-by-k Addition. For experiments in the range of [0,9], we consider $k \in \{-2, -1, 1, 2\}$. For experiments in the range of [0,99] and [0,999], we consider $k \in \{-10, -9, ..., -1, 1, 2, ..., 10\}$. We have reported the results in Fig. 12-13, incorporating the range and offset information. We use 16 shots in the experiments in Fig. 6(a).

Shifted Multiple-choice QA. We focus on 6 subjects in the MMLU dataset (Hendrycks et al., 2021): high school government and politics, high school US history, US foreign policy, marketing, high school psychology, sociology. We downloaded the MMLU dataset from hendrycks/test. We chose these subjects because `Gemma-2 (9B)` achieves 90% accuracy with 5 shots on them. For subjects where `Gemma-2 (9B)` achieves lower accuracies, tracking and analyzing performance on Shift-by-One MMLU becomes challenging, because the model could score points by random guessing. We use 16 shots in the experiments in Fig. 6(b), where the 16 shots combine "validation" and "dev" examples from the MMLU dataset.

Caesar Cipher. We adopted a cyclic approach where "a" is considered the next character after "z". We also included both lower-case or upper-case examples, *e.g.*, "c -> d" and "C -> D" are both valid examples in ROT-1. We use 16 shots in the experiments in Fig. 6(c).

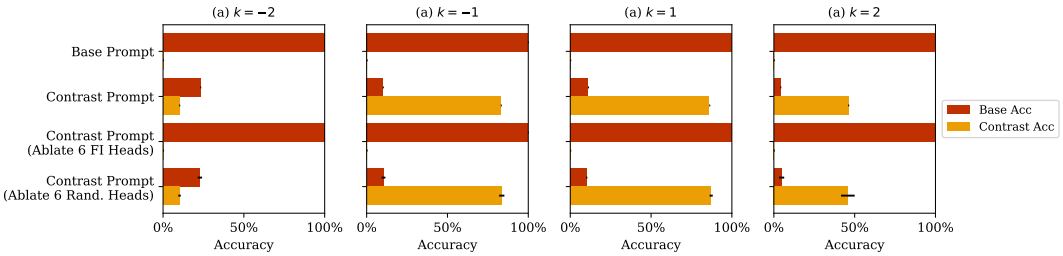

Figure 28: **Task Generalization with FI Heads, Off-by-k Addition.** We consider addition in the range of [0,9] and $k \in \{-2, -1, 1, 2\}$.

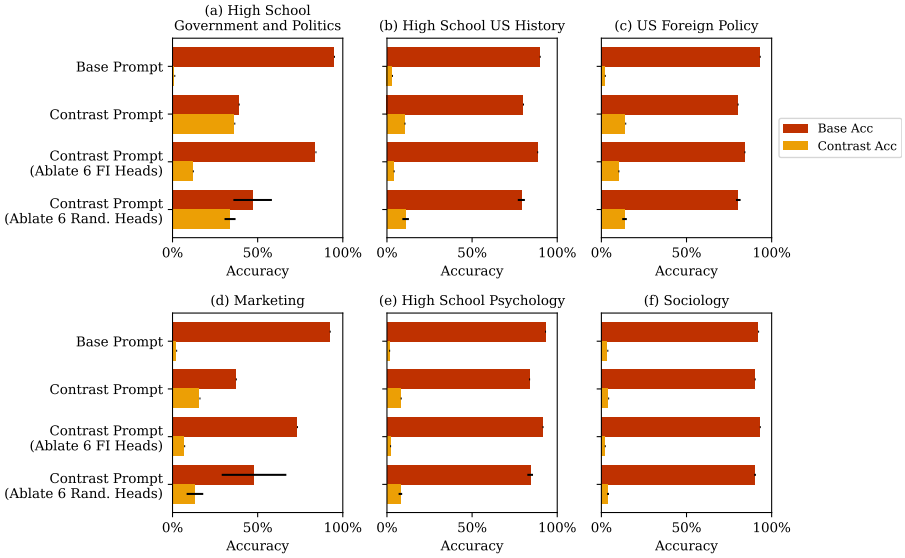

Figure 29: **Task Generalization with FI Heads, Shifted MMLU.**

In the early stages of this work, we experimented with multi-character Caesar cipher. To prevent multiple characters from being tokenized as a single unit (*e.g.*, "ew" as one token in `Gemma-2`'s tokenizer), we used a preceding whitespace (␣) before each character, formatting it as "␣e␣w" so that "␣e" and "␣w" became separate tokens. However, we ultimately focused on one-character Caesar cipher in the experiments because `Gemma-2 (9B)` has insufficient performance on the multi-character version. The tokenization-aware formatting was retained. The actual model input will be "␣c -> ␣d" for the example "c -> d".

Base-k Addition. We sampled two-digit addition problems using a procedure similar to off-by-k addition, with one additional constraint that the sum number c has two digits in both base-10 and base-k. We use 32 shots in the experiments in Fig. 6(d). For the base-8 addition analysis in §5.2 and Table 3, examples for Case 1-3 were resampled.

G.2 Results

Full Results using Different Offsets and Bases. Previously in Fig. 6, we report results on representative cases, *e.g.*, $k = 2$ in off-by-k addition, the subject of "high school government and politics" in shifted MMLU. In Fig. 28-31, we report results of the full list of offsets and subjects.

We observe that some of these task variants exceed `Gemma-2 (9B)`'s capabilities. For instance, `Gemma-2 (9B)` has notable performance on cipher when $k \in \{-2, -1, 1, 2, 3, 13\}$ but shows insufficient performance in other settings. Similarly, it only exhibits non-trivial performance on certain subjects of Shifted MMLU. However, when models do have non-trivial performance, we consistently see the involvement of the FI heads, evidenced by the decreased contrast accuracy after ablating them.

Figure 30: **Task Generalization with FI Heads, Caesar Cipher.** We consider $k \in \{-12, -11, ..., -1\}$ and $\{1, 2, ..., 13\}$. In this figure, we ablate 6 FI heads plus 3 additional FI heads (discussed in §4 and Fig. 5), yielding a clearer pattern than ablating 6 heads alone.

Ablating three additional FI Heads. Previously in Fig. 6, we ablate the 6 FI heads we identified in §3.2 by setting a threshold of $|r| > 2\%$. In §4 and Fig. 5 we showed that 3 additional FI heads with weaker effect ($1\% < |r| < 2\%$) also contribute meaningfully to off-by-one addition. Here we consider repeating the experiments on task generalization in Fig. 6 and ablating the 9 heads together. We report the results in Fig. 32.

We find that the 3 weaker heads contribute meaningfully to the Shifted MMLU, causing its contrast performance to drop to near 0% when all 9 heads are ablated (Fig. 32(b)), contrasting with 12% when 6 heads are ablated (Fig. 6(b)). We have a similar observation with Caesar Cipher ($k = 2$), where contrast accuracy drops to 0% in (Fig. 32(c)), contrasting with 36% when 6 heads are ablated (Fig. 6(c)). These observations suggest that the 3 heads may specialize in letters more than numbers. Understanding these detailed specializations will be an interesting direction for future work.

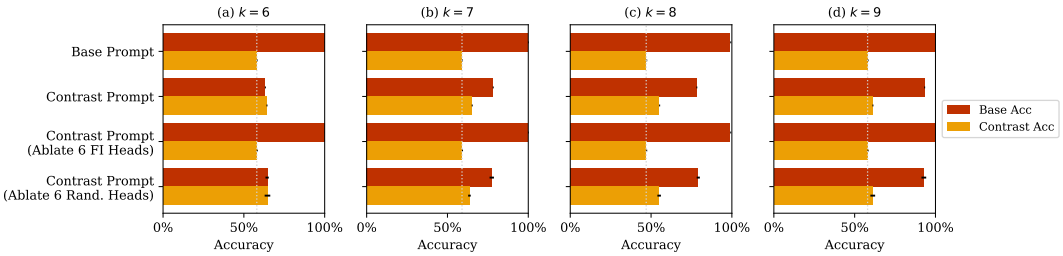

Figure 31: **Task Generalization with FI Heads, Base-k Addition.** We consider $k \in \{6, 7, 8, 9\}$. The dashed lines represent the base prompt's contrast accuracy, emphasizing the delta in contrast accuracies between rows.

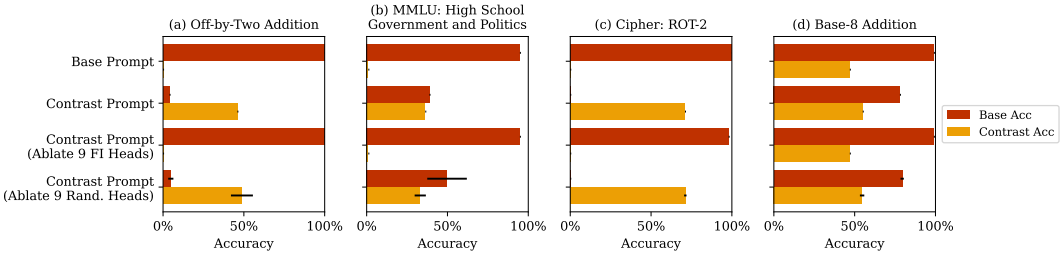

Figure 32: **Task Generalization with FI Heads, Ablating 9 FI Heads.** We repeat the experiment in Fig. 6, this time ablating three additional FI heads (H32.4, H28.6, H24.9) which showed a weaker effect ($1\% < |r| < 2\%$) during circuit discovery on off-by-one addition.

H Reproducibility

Frameworks. We primarily use the `transformer-lens` (Nanda & Bloom, 2022) library for model inference and interpretability analysis. This library is built on the `transformers` (Wolf et al., 2020) library. We have also used the `llm-transparency-tool` (Ferrando & Voita, 2024; Tufanov et al., 2024) for early exploration.

Hardware. All experiments were conducted with one NVIDIA RTX A6000 GPU (48GB). Path patching experiments involving 100 4-shot examples and iterating over all attention heads for a given target node will typically take 2 hours.

Code Release. Our code can be found at `INK-USC/function-induction`.